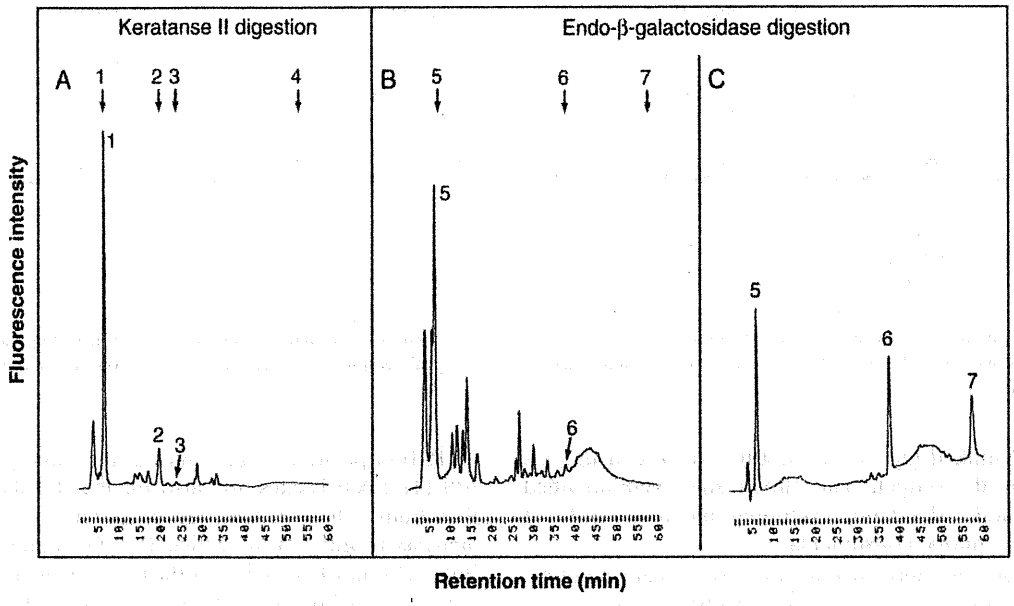

Fig. 7. HPLC profiles of keratan sulfate-derived oligosaccharides. (**A**) The R-10G antigen was digested with keratanase II and the digests were submitted to HPLC as described under Materials and methods. (**B**) The R-10G antigen was digested with endo-β-galactosidase and the digests were submitted to HPLC as in (**A**). (**C**) A standard keratan sulfate from bovine cornea was digested with endo-β-galactosidase and the digests were submitted to HPLC as in (A). Arrows: 1, Gal-GlcNAc(6S); 2, Gal-GlcNAc(6S)-Gal-GlcNAc(6S); 3, Gal(6S)-GlcNAc(6S); 4, Gal(6S)-GlcNAc(6S)-Gal(6S)-GlcNAc(6S); 5, GlcNAc(6S)-Gal; 6, GlcNAc (6S)-Gal(6S)-GlcNAc(6S)-Gal; 7, GlcNAc(6S)-Gal(6S)-GlcNAc(6S)-Gal(6S)-GlcNAc(6S)-Gal.

a considerable level of oversulfated structure (sulfation at C-6 of Gal residues) in the keratan sulfate from bovine cornea and in contrast by a negligible level of this sulfation in the R-10G epitope. This is in accordance with a substantially higher sulfation index of the keratan sulfate from bovine cornea, 1.29, than that of the R-10G antigen, 1.02, as described above. It is possible that several significant peaks between peak 5 and peak 6 in Figure 7B may represent additional modifications such as fucosylation, sialylation or something else of Gal residues in the keratan sulfate in the R-10G antigen.

Taking all these results into account, it is reasonable to conclude that the R-10G epitope is a unique keratan sulfate lacking oversulfated structures.

Characterization of R-10G epitopes by ELISA

In this experiment, the binding activity of R-10G toward the biotinylated GAG specimens, which had been fixed to the streptavidin-coated plastic wells, was assayed using an enzyme-linked immunosorbent assay (ELISA) system in comparison with that of 5D4, which is known to recognize a high-sulfated keratan sulfate (Mehmet et al. 1986). As shown in Figure 8A, the keratan sulfate from bovine cornea reacted effectively with R-10G, while the other GAGs, hyaluronic acid, chondroitin, chondroitin sulfate from whale cartilage, chondroitin sulfate from the spinal column of *Acipenser mediros-tris*, chondroitin sulfate B, chondroitin sulfate C, chondroitin sulfate D, chondroitin sulfate E and heparan sulfate, did not show any significant binding activity toward R-10G, indicating clearly that the binding specificity of R-10G is very strict for keratan sulfate. In this respect, R-10G is similar to 5D4 (Figure 8B). It should be noted, however, that there is >100-fold difference in the amount of antibodies required to generate adequate responses between these two antibodies, 0.008 μg/mL for 5D4 and 1 μg/mL for R-10G. This may indicate that the keratan sulfate from bovine cornea is abundant in the 5D4 epitope but is scarce in the R-10G epitope. A marked difference between R-10G and 5D4 was also demonstrated by inhibition studies.

As shown in Figure 8C, the binding of R-10G to the keratan sulfate from bovine cornea in the plastic plates was inhibited by the same keratan sulfate in proportion to the amount of the keratan sulfate added to the incubation mixture, as expected. In contrast, a high-sulfated keratan sulfate (KSP-1), which was isolated from shark cartilage according to the procedure as described by Furuhashi (Furuhashi 1961), did not inhibit the R-10G binding at all, indicating the inability of R-10G to bind to a high-sulfated keratan sulfate. On the other hand, as shown in Figure 8D, a highly sulfated-keratan sulfate (KSP-1) inhibited the 5D4 binding approximately 100 times more than that of the keratan sulfate from bovine cornea, confirming the highly specific binding of 5D4 to a high-sulfated keratan sulfate (Mehmet et al. 1986).

In the next experiment, when the keratan sulfate fixed on a well was digested with keratanase II, the R-10G binding activity disappeared almost completely (Figure 8E), as the 5D4 binding activity did (Figure 8F). When the keratan sulfate was digested with keratanase, the R-10G binding activity disappeared again almost completely (Figure 8E), while the 5D4 binding activity was reduced only partially (~40%) (Figure 8F). This differential susceptibility to keratanase between the R-10G and 5D4 epitopes is most probably due to the substrate specificity of keratanase, which digests the keratan sulfate only when C-6 of the GalNAc is sulfated but C-6 of the galactose residue is not sulfated (Ito et al. 1986)

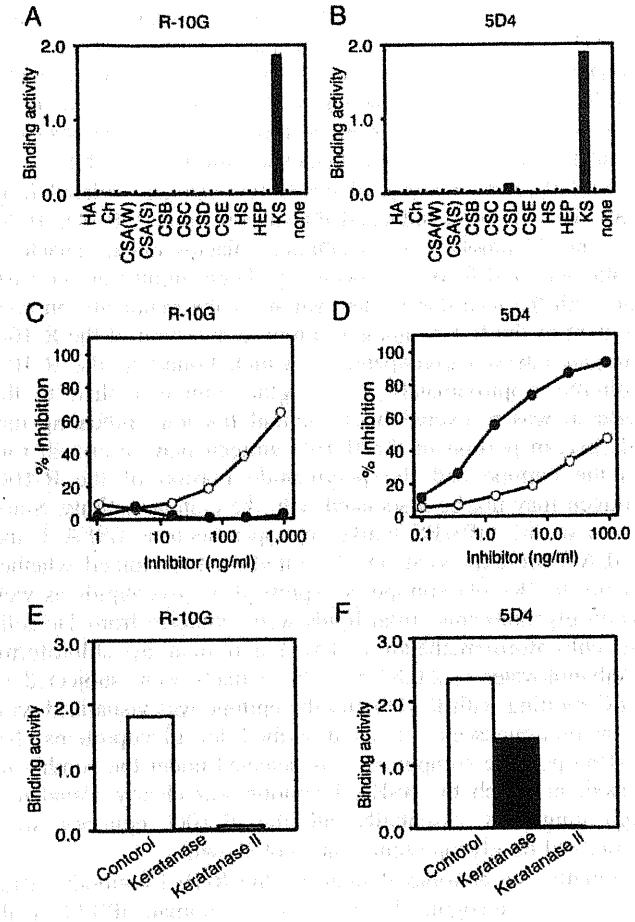

Fig. 8. Characterization of the R-10G epitope by ELISA. (**A**) Binding activities of R-10G toward various GAGs were determined. GAGs used: HA (hyaluronic acid), Ch (chondroitin from shark cartilage), CSA (W) (chondroitin sulfate from whale cartilage), CSA (S) (chondroitin sulfate from the spinal column of *Acipenser medirostris*), CSB (chondroitin sulfate B), CSC (chondroitin sulfate C), CSD (chondroitin sulfate D), CSE (chondroitin sulfate E), HS (heparan sulfate) and KS (keratan sulfate). IgG1 from murine myeloma was added to the GAG-coated plates and the amounts of IgG1 bound to the plates were determined as negative controls. (**B**) Binding activities of 5D4 toward various glycosaminoglycans were determined as described in (**A**). (**C** and **D**) Inhibitory effects of two keratan sulfates from different origins on the antibody binding to keratan sulfate from bovine cornea. To assay mixtures containing R-10G (**C**) or 5D4 (**D**), increasing amounts of KS (keratan sulfate from bovine cornea) (open circle) or KPS-1 (high-sulfated keratan sulfate form shark cartilage) (filled circle) were added, and the effects of these inhibitors on the binding activity were determined as described in (**A**). (**E** and **F**) Different sensitivities of the R-10G and 5D4 epitope structures to keratan sulfate-degrading enzymes. Biotinylated keratan sulfate from bovine cornea, which had been treated with either no enzyme (white bars), keratanase (black bars), or keratanase II (dashed bars) at 37°C overnight, was fixed on a streptavidin-coated plate (1 μg/mL), and the binding activity of R-10G (1 μg/mL) (**E**) or 5D4 (0.008 μg/mL) (**F**) to the residual oligosaccharide moieties on the plates were assayed as described in (**A**).

(see Figure 6). The 5D4 epitope is a high-sulfated keratan sulfate, and C-6 of the galactose linked to GalNAc is frequently sulfated and resistant to keratanase digestion. Conversely, these results suggested that C-6 of the galactose residues in the R-10G epitope is mostly not sulfated.

Finally, these studies involving an exogenous keratan sulfate and 5D4 antibodies confirmed strongly the conclusions made with the endogenous antigen molecule on hiPS cells and R-10G, as described above.

Tissue distribution of the R-10G epitope

Conventional hiPS/ES/EC marker antibodies are expressed not exclusively on hiPS/ES/EC cells but the same or cross-reactive epitopes are occasionally expressed either in fetal or adult tissues. For example, TRA-1-81 reacted with human mammary ducts, stomach, the small and large intestine and others, and TRA-1-60 reacted with human smooth muscle cells, the intestine, lung, skin, uterus and others, in addition to hEC cells (Andrews et al. 1984). In this connection, we examined the tissue distribution of the R-10G epitope by immunohistochemistry studies of human adult and fetal tissues using a human tissue array. Out of 32 human adult and fetal tissues tested, adult brain and adult cerebellum showed strong reactivity to R-10G, which are comparable to that for Tic cells. In contrast, the other adult and fetal tissues, that is, placenta, bladder, brain (fetal), cerebellum (fetal), colon, heart, kidney, liver, lung, skin, skeletal muscle, small intestine, spleen, stomach, thymus and tongue did not show any significant staining to the R-10G except for the fetal liver, in which weak spots like islets were detected. Thus, the molecules recognized by R-10G are not confined to hiPS/ES cells but they are expressed on a very limited number of tissues in a unique fashion. In agreement with this staining profile of human tissues, the keratan sulfate isolated from the mouse brain and the rat brain were shown to have sulfation indexes of 1.04 and 1.08, respectively (Oguma et al. 2001), which are close to that of the R-10G antigen on hiPS cells, 1.02.

Discussion

We have established a monoclonal antibody, R-10G, which is a unique iPS/ES marker antibody distinguishing hiPS cells (normal cells) and hEC cells (teratoma cells). Using an affinity column of the R-10G antibody, the R-10G antigen molecule was isolated from hiPS cells and subjected to characterization from various aspects.

The initial characterization of the glycan epitope of R-10G on the hiPS cell surface was carried out with western blotting by comparing the R-10G antigen profiles before and after glycosidase digestion. Of the various glycosidases tested, keratanase II, keratanase and endo-β-galactosidase, all known to degrade keratan sulfate, abolished the R-10G positive band almost completely, indicating that the epitope is a keratan sulfate. However, 5D4, the most widely used keratan sulfate-recognizing monoclonal antibody, did not bind to hiPS cells, as seen on immunocytochemical staining (data not shown). In addition, on western blotting, neither Tic cell lysates nor the R-10G antigen isolated therefrom gave any detectable bands with 5D4 (data not shown). Considering the fact that 5D4 recognizes a high-sulfated keratan sulfate (Mehmet et al. 1986), it was reasonable to assume that the R-10G epitope belongs to a type of keratan sulfate, whose level of oversulfation is low for a keratan sulfate. This assumption was confirmed by ion-pair reverse-phase HPLC

analysis of the digestion products of the R-10G antigen with keratanase II and endo-β-galactosidase. Upon keratanase II digestion, the glycans on the R-10G antigen molecule were shown to be degraded almost completely to the disaccharide-repeating unit of keratan sulfate, Gal-GlcNAc (6S), in parallel with the abolishment of the antibody binding activity, suggesting strongly that the R-10G epitope consists of Gal-GlcNAc(6S) or its tandem repeat structures. This conclusion was confirmed further by the identification of the major component of the endo-β-galactosidase digests as GlcNAc(6S)-Gal. The analysis of the endo-β-galactosidase digests indicated also that there is little sulfation at C-6 of the galactose residues, if any. The sulfation index of the R-10G antigen was calculated to be 1.02. This figure is significantly lower than that of keratan sulfate from bovine cornea, 1.20, and much lower than that of keratan sulfate from bovine cartilage, 1.57 (Oguma et al. 2001). The lack of oversulfation in the R-10 antigen was further confirmed by an ELISA study involving biotinylated keratan sulfate from bovine cornea, which had been fixed on avidin-coated plates as described above.

Taken these results together, it may be reasonable to propose that the R-10G epitope consists of the basic repeating unit of keratan sulfate, Gal-GlcNAc(6S), or its tandem repeat with few oversulfation, which are frequently observed at C-6 of galactose residues in many other keratan sulfates from various origins. However, it is clear that the exact sequence of the R-10G epitope remains to be elucidated and further studies using latest technologies such as glycan sequencing with LC/MS/MS and epitope profiling with carbohydrate microarray platform will be pursued. In this regard, it would be interesting to refer to a recent report (Natunen et al. 2011) that TRA-1-60 and TRA-1-81 require Galβ1-3GlcNAcβ1-3Galβ1-4GlcNAc (a dimeric type 1 lactosamine structure) as a minimum epitope.

Since R-10G, TRA-1-60 and TRA-1-81 share a common carrier protein and the affinity-purified R-10G antigen reacted not only with R-10G but also with TRA-1-60 and TRA-1-81 (Schopperle and DeWolf 2007), the structural relationship between these three immunogenic glycoproteins was speculated. Upon western blotting of the R-10G antigen and Tic cell lysates, slight but significant differences were detected in the migration positions of the respective antibody-reactive bands; they decreased successively in the order of R-10G, TRA-1-60 and TRA-1-81 with some overlapping (see Figure 5A), suggesting that either the size or the number of glycan chains carrying the R-10G epitope may be larger than that of those carrying the TRA-1-60 or the TRA-1-81 epitope. Significant differences were also detected in the relative intensities of the bands of the R-10G antigen as to the corresponding bands of the Tic cell lysates; the ratio decreased from R-10G to TRA-1-60 through TRA-1-81. The R-10G epitope-carrying podocalyxin was most effectively adsorbed to a column, indicating the immunological distinctiveness of these epitopes. The column less effectively captured particularly the TRA-1-60 epitope. The precise glycan structures of these epitopes remain to be elucidated, but the TRA-1-60 and TRA-1-81 epitopes probably belong to a type of keratan sulfate similar to the R-10G epitope, because 5D4, an antibody recognizing a high-sulfated keratan sulfate and BCD4, another commercially available antibody recognizing keratan sulfate, did not bind to hiPS/ES cells (R-10G/TRA-1-60/TRA-1-81 reacting cells) (data not shown), although these epitopes were susceptible to digestions with keratan sulfate-degrading enzymes in vitro (Figure 5B).

Carbohydrate analysis of the R-10G antigen isolated from 1.0×10^6 Tic cells indicated that it contained 370, 84, 1026, 46 and 51 pmol of glucosamine, galactosamine, galactose, sialic acid and fucose, respectively. These figures are consistent with the idea that keratan sulfate is the major glycan constituent of the R-10G antigen. Pronase digestion of the R-10G antigen released glycopeptides, which bound to the R-10G column. Approximately 2/3 of glucosamine applied to the column was recovered in the bound fraction, indicating that the glycan portion of the R-10G antigen plays a crucial role as the epitope and the polypeptide portion of the R-10G antigen may not be associated with the epitope activity. Since some of the hiPS/ES marker epitopes such as SSEA-3 and SSEA-4 are expressed on glycolipids, we examined whether or not the R-10G epitope is expressed on glycolipids as well as on glycoproteins. Total lipids were extracted from Tic cells by chloroform/methanol (2:1 v/v) and then by chloroform/methanol/water (1:2:0.8 v/v). The extracts were subjected to TLC blotting with R-10G and the epitope was visualized with a chemiluminescent kit as described for glycoproteins. No R-10G positive component was detected under the conditions tested, in which the SSEA-4 epitope was clearly visualized, indicating that essentially all the R-10G epitopes were expressed on glycoproteins (data not shown).

Finally, the epitopes defined by the R-10G antibody differ from those recognized by the other human iPS/ES cell-specific antibodies and from other keratan sulfate-recognizing antibodies that had been described and provide a new marker for studying the roles of glycans on the surface of hiPS/ES cells in the maintenance of self-renewal and pluripotency and during the process of differentiation, but also as a potent tool for the evaluation and standardization of hiPS cells with different tissue origins and different histories in regenerative medicine. Furthermore, the R-10G antibody might be useful in studies of cancer biology, since the lack of the R-10G epitope on tumor cell surfaces may be somehow relevant to the aberrant properties of tumor cells.

Materials and methods

Materials

Antibodies. Anti-human TRA-1-60 (clone # TRA-1-60, mouse IgM), anti-human TRA-1-81 (clone # TRA-1-81, mouse IgM) and anti-human/mouse SSEA-4 (clone # MC813, mouse IgG3) antibodies were obtained from Santa Cruz Biotechnology (Santa Cruz, CA), and anti-human/mouse SSEA-1 (clone # MC480, mouse IgM), and anti-human/mouse SSEA-3 (clone # MC631, rat IgM) antibodies were obtained from R&D Systems (Minneapolis, MN). Anti-keratan sulfate antibodies, clone # 5D4 (mouse IgG1) and clone # BCD4 (mouse IgG1) were obtained from Seikagaku Biobusiness (Tokyo, Japan).

Glycosaminoglycans. Keratan sulfate from bovine cornea, keratan sulfate from shark cartilage, hyaluronic acid from pig skin, chondroitin from shark cartilage, chondroitin sulfate from whale cartilage, chondroitin sulfate from the spinal column of *Acipenser medirostris*, chondroitin sulfate B from pig skin, chondroitin sulfate C from shark cartilage, chondroitin sulfate D from shark cartilage, chondroitin sulfate E from squid cartilage and heparan sulfate from bovine kidney were obtained from Seikagaku Biobusiness.

Enzymes. PNGase F (recombinant protein from *Escherichia coli*) was obtained from Roche Diagnostics GmbH (Mannheim, Germany), neuraminidase (*Arthrobacter ureafaciens*) from Nacalai Tesque (Kyoto, Japan), neuraminidase (*Vibrio cholerae*) from Roche Diagnostics GmbH, α1–3/4 fucosidase from Takara Bio (Shiga, Japan), α1–2 fucosidase from New England Biolabs (Ipswich, MA). Chondroitinase ABC (*Proteus vulgaris*), a heparinase mix (a mixture of heparinase, heparitinase I and heparitinase II), keratanase (*Pseudomonas* sp.), keratanase II (*Bacillus* sp.) and endo-β-galactosidase (*Escherichia freundii*) were from Seikagaku Biobusiness. Pronase (*Streptomyces griseus*) was obtained from Merck Millipore (Billerica, MA).

Cells and cell culture. HiPS cell lines: Tic (JCRB1331) and Squeaky (JCRB1329), which were generated from MRC-5 (Toyoda et al. 2011), human embryonic lung fibroblasts, by transduction of four defined factors: Oct3/4, Sox2, Klf4 and c-Myc (Takahashi et al. 2007), were obtained from the Japanese Collection of Research Bioresources (JCRB), National Institute of Biomedical Innovation (Osaka, Japan). 201B7 were provided by the Center for iPS Cell Research and Application (CiRA), Kyoto University (Kyoto, Japan). Human ES cell lines, H9 (WA09), were obtained from the Wisconsin International Stem Cell (WISC) Bank, WiCell (Madison, WI), and KhES-3 was provided by the Institute for Frontier Medical Sciences, Kyoto University (Kyoto, Japan). These cells were maintained in KSR-based medium that consisted of KNOCKOUT DMEM/F-12 (400 mL, Invitrogen-Life Technologies, Carlsbad, CA), MEM nonessential amino acids solution (4.0 mL, Invitrogen-Life Technologies), 200 mM L-glutamine (5.0 mL), KNOCKOUT Serum Replacement (100 mL, Invitrogen-Life Technologies), 55 mM 2-mercaptoethanol (0.925 mL) and human basic fibroblast growth factor (bFGF, Sigma-Aldrich, St. Louis, MO) on mitomycin C-inactivated mouse embryonic fibroblasts (MEF, Merck Millipore), in 25 cm^2 flask (Corning, Corning, NY) at 37°C/5% CO_2. Human EC cell line 2102Ep was a generous gift from Prof. Peter Andrews (University of Sheffield) to National Institute of Biomedical Innovation (NIBIO), and NCR-G3 (JCRB1168) was obtained from JCRB. MRC-5 (JCRB9008), a fibroblast-like cell line derived from human lung tissue of a 14-week-old male fetus, was obtained from JCRB. H9 and 2102Ep were cultured only in NIBIO following the Guidelines for Derivation and Utilization of hES Cells of the Ministry of Education, Culture, Sports, Science and Technology of Japan. Furthermore, the study was approved by Independent Ethics Committee of NIBIO. A human tissue array was obtained from BioChain Institution, Inc. (Hayward, CA).

Preparation of monoclonal antibodies recognizing hiPS cells

Preparation of hiPS cells for immunization and screening. An hiPS cell line, Tic, was used as the immunogenic antigen and also as the screening probe. Tic cells cultured in KSR-based medium on MEF were then transferred to a growth factor defined serum-free culture medium hESF9, described previously (Furue et al. 2008). HESF9 medium comprised ESF basal medium without HEPES with L-ascorbic acid 2-phosphate (hESF-grow, Cell Science and Technology Institute, Sendai, Japan) (Furue et al. 2005) supplemented with six-factors (human recombinant insulin, human apotransferrin, 2-mercaptoethanol, 2-ethanolamine, sodium selenite and oleic acid conjugated with fatty acid-free bovine serum albumin (FAF-BSA)), heparin sulfate sodium salt and human bFGF. After culturing at 37°C for 2 days, the undifferentiated hiPS cells ($3 \times 10^5 \sim 1 \times 10^6$ cells/25 cm^2 flask) were harvested by treatment with 0.1% ethylenediaminetetraacetic acid (EDTA)-4Na/phosphate-buffered saline (PBS), washed with PBS and stored at −80°C until just before use as the immunogen. For screening, the cells, which had been incubated with ROCK inhibitor (10 μM, Y27632; Wako Pure Chemical Industries, Osaka, Japan) (Watanabe et al. 2007) for 1 h, were harvested with ACCUTASE™ (1 mL; Merck Millipore), washed with KSR-based medium, resuspended in hESF9 medium and then seeded on fibronectin-coated 96-well plates (5×10^3 cells/well; BD, Franklin Lakes, NJ). After 4 days of culture, cells were fixed with 1% acetic acid/ethanol (100 μL/well) for 10 min at room temperature. After washing with PBS, the plates were stored at −80°C until just before use.

Immunization. Two different protocols were used for the immunization of mice with hiPS cells. In protocol A, freeze-thawed Tic cells (1.5×10^7 cells in 0.5 mL PBS) were emulsified with an equal volume of Freund's Complete Adjuvant (FCA, Thermo Fisher Scientific, Rockford, IL), and then injected into three 8-week-old female C57BL/6 mice (200 μL/mice) intraperitoneally on Day 0, followed by a booster injection on Day 25, and the mice were sacrificed on Day 28. In protocol B, an FCA emulsion of Tic cells was injected subcutaneously into three mice (200 μL/mice) and the mice were sacrificed after 2 weeks.

Cell fusion and cloning. Lymphocytes from the spleens of the protocol A mice and lymph nodes from the protocol B mice were mixed and fused with P3U1 mouse myeloma cells using polyethylene glycol. Fused cells were seeded onto ten 96-well tissue culture plates, and hybridomas were selected by adding the hybridoma medium (S-Clone cloning medium CM-B containing hypoxanthine, aminopterin and thymidine (HAT); Sanko Junyaku, Tokyo, Japan). On Day 7 after plating, the first screening was performed using Tic cell-fixed plates. The culture supernatant from each hybridoma was added to Tic cell-fixed screening plates, which had been pretreated with a blocking solution containing 0.1% H_2O_2 (Blocker Casein; Pierce-Thermo Fisher Scientific) overnight. The hybridoma culture supernatant was incubated on the cell plates at room temperature for 2 h. After washing the plates with PBS, 1:2000-diluted horseradish peroxidase (HRP)-conjugated

anti-mouse IgG (Takara Bio) was added to each well, followed by incubation for 1 h. After final washing, 3,3′-diaminobenzidine (DAB) (Metal Enhanced DAB Substrate Kit (Pierce-Thermo Scientific)) was added to the plates and coloring was allowed to proceed for 10–15 min, followed by observation of the stained plates under a light microscope (Olympus IX 7, Olympus, Tokyo, Japan). The hiPS-positive antibody-producing hybridomas were then subjected to the second cell screening, in which human hEC cells (2102Ep), human fibroblasts (MRC-5) and MEF cells were used as probes as well as hiPS cells (Tic). The isotypes of antibodies were examined by using a mouse monoclonal antibody isotyping test kit (AbD Serotec, Kidlington, UK).

Purification of the R-10G antibody from mouse ascites fluid. The R-10G hybridoma cell line was injected intraperitoneally into pristane-treated SCID mice (CB-17/Icr-scid Jcl). Two weeks later, the ascites fluid (2.5 mL) was collected from the mice and applied to a Protein A-Sepharose column (1 × 6.0 cm) (GE Healthcare, Buckinghamshire, UK). The R-10G antibody bound to the column in 1.5 M glycine-NaOH buffer, pH 8.9/3 M NaCl was eluted with 0.1 M citric acid-phosphate buffer, pH 4.0. The eluate containing the R-10G antibody (IgG1) was immediately neutralized to pH 7–8 by adding 3 M Tris–HCl buffer, pH 9.0.

Immunocytochemistry

Imaging analysis. Cells seeded onto 24-well plates were fixed in 4% paraformaldehyde (PFA) at room temperature for 15 min, blocked with 3% fetal bovine serum (FBS) (ES cell-qualified; Invitrogen-Life Technologies)/PBS for 1 h and then incubated with primary antibodies (R-10G (10 μg/mL), TRA-1-60 (2 μg/mL), TRA-1-81 (2 μg/mL), SSEA-1 (5 μg/mL), SSEA-3 (5 μg/mL) and SSEA-4 (2 μg/mL)) at 4°C overnight. After washing with PBS three times each for 5 min, localization of antibodies was visualized by incubation with Alexa Fluor 647-conjugated chicken anti-mouse IgG (Invitrogen-Life Technologies) as the second antibody at room temperature for 1 h, followed by fixing the cells with 0.1%Triton-X100/4%PFA and then staining with Hoechst 33342 (1:5000 in PBS, Dojindo Laboratories, Kumamoto, Japan). The cells were imaged with an InCell Analyzer 2000 (GE Healthcare, Buckinghamshire, UK) and quantitated with Developer Toolbox ver1.8.

Laser confocal scanning microscopy. Cells were seeded with MEF onto gelatin-coated 4-well plastic chamber (Millipore EZ slides (Millipore, Billerica, MA)). After 3–5 days of culture, the cells were fixed in 4% PFA at room temperature for 10 min, blocked with 3% FBS/PBS for 1 h and then incubated with R-10G (10 μg/mL, as the first primary antibody) at 4°C overnight. After washing with 0.1% PBS three times, the cells were incubated with Alexa Fluor 488-conjugated goat anti-mouse IgG1 as the secondary antibody in 1% FBS/PBS at room temperature for 30–60 min. For double staining with the second primary antibody (TRA-1-60 or TRA-1-81, 2 μg/mL), cells were washed and blocked in the same way as described above and then incubated with the second primary antibody at 4°C overnight. Then, the cells were incubated with Alexa Fluor 555-conjugated goat anti-mouse IgM as the secondary antibody as described above. After washing with 0.1% FBS/PBS three times, the cells were fixed with 0.1% Triton X-100/4% PFA at room temperature for 10 min, followed by staining with TO-PRO3 (1:500 in PBS, Invitrogen-Life Technologies) and monitored under a confocal laser scanning microscope FV1000 (Olympus, Tokyo, Japan).

Isolation of R-10G antigens from hiPS cells

Human iPS cell lysates were prepared by dissolving Tic cells (1.25 mg protein/1 × 10^7 cells, as determined with a Micro BCA protein assay kit (Pierce-Thermo Scientific)) in the complete RIPA buffer (0.5 mL) under sonication. This buffer consists of RIPA lysis buffer (6 mM Tris–HCl, pH 8.0, 1% Nonidet P-40, 0.5% sodium deoxycholate, 0.1% SDS, 0.004% sodium azide), protease inhibitor cocktail, 2.5 mM PMSF and 1 mM sodium orthovanadate (Santa Cruz Biotechnology). The lysate was centrifuged to remove insoluble residues and the supernatant was applied to an R-10G-Sepharose 4B column (gel volume, 0.4 mL), which had been prepared by coupling R-10G (4 mg protein) to BrCN-activated Sepharose 4B (1.0 mL; GE Healthcare) in 0.1 M $NaHCO_3$ buffer, pH 8.3/0.5 M NaCl according to the manufacturer's instructions. After washing the column with the complete RIPA lysis buffer, the protein bound to the column was eluted with an eluting buffer consisting of RIPA buffer (1:10 diluted), protease inhibitor cocktail, PMSF, sodium orthovanadate and 0.1 M diethylamine (pH 11.5). The eluate containing the R-10G antigen was immediately neutralized by adding 1 M Tris–HCl buffer, pH 6.8. In some experiments, the R-10G-Sepharose 4B column was washed with 0.1% Nonidet P-40/20 mM Tris–HCl, pH 7.4/150 mM NaCl, and the protein bound to the column was eluted with 0.1% Nonidet P-40/10 mM Tris–HCl, pH 7.4/150 mM NaCl/0.1 M diethylamine, pH 11.5.

SDS-PAGE and western blotting

SDS–PAGE and western blotting were performed according to the methods of Laemmli (1970) and Towbin et al.(1992). Briefly, samples were resolved by electrophoresis on a 4–15% gradient SDS-polyacrylamide gel (Mini-PROTEAN TGX-gel; Bio-Rad Laboratories, Hercules, CA) under nonreducing conditions unless otherwise stated, followed by either western blotting or protein staining. For western blotting, resolved proteins were transferred to Immobilon Transfer membranes (Merck Millipore), followed by immunoblot detection with R-10G (3 μg/mL), TRA-1-81 (1 μg/mL) or TRA-1-60 (1 μg/mL). For visualization, a chemiluminescent substrate kit (Pierce-Thermo Scientific) was used with HRP-conjugated rabbit anti-mouse immunoglobulin (Dako Cytomation, Denmark A/S), followed by analysis with a Lumino-Image Analyzer, Las 4000 mini (GE Healthcare). Protein was stained with Coomassie brilliant blue G-250 (Gel Code Blue; Invitrogen-Life Technologies).

Identification of the R-10G antigen protein

Following SDS–PAGE, gels were stained with SYPRO Ruby Protein Gel Stain (Invitrogen-Life Technologies), and protein bands corresponding to the western blotting bands were

excised from the gel and subjected to *in gel* trypsin digestion. The peptides extracted from the gel pieces were analyzed by LC/MS/MS using a liquid chromatography instrument (Paradigm MS4 HPLC system; Michrom Bioresources, Auburn, CA) equipped with a linear ion trap type mass spectrometer (LTQ; Thermo Fisher Scientific, Waltham, MA). A reversed-phase column (L-column Micro; 150 × 0.075 mm, 3 μm; Chemicals Evaluation and Research Institute, Tokyo, Japan) was used as the analytical column, the eluents being 2% CH_3CN containing 0.1% formic acid (Pump A) and 90% CH_3CN containing 0.1% formic acid (Pump B). The peptides were eluted at a flow rate of 300 nL/min with a gradient of 2–65% of B buffer in 50 min. Data-dependent MS/MS acquisition was performed for the most intense ions as precursors. The spectrum data obtained on LC/MS/MS were subjected to database search analysis with the TurboSEQUEST algorithm (BioWorks 3.1; Thermo Fisher Scientific) by using the UniProt database. The static modification of carboxymethylation (58.0 u) at Cys was used as the modified parameters for database search analysis. The SEQUEST criterion, known as Xcorr vs. Charge State, was set to 1.5(+1), 2.0(+2), 2.5(+3) and 3.0 (+4) for the protein identifications.

Glycosidase digestions for western blotting

The reaction mixtures consisting of the cell lysates (~12 μg protein, corresponding to 1×10^5 cells) or the R-10G antigen (corresponding to ~1×10^5 cells) in complete RIPA buffer were digested with various glycosidases under the conditions given below, and the digests were subjected to SDS–PAGE and western blotting. In some experiments, when the solvent for R-10G antigens (RIPA buffer) inhibited the intended enzyme activity, the RIPA buffer was replaced with 0.1% Nonidet P-40/10 mM Tris–HCl, pH 7.4/150 mM NaCl by using an R-10G-Sepharose 4B column (gel volume; 0.4 mL). For chondroitinase ABC digestion, the R-10G antigen was digested with 2 mU of chondroitinase ABC in 20 μL of 50 mM Tris-acetate buffer, pH 8.0, at 37°C for 18 h. For heparinase mix digestion, the R-10G antigen was digested with 6 mU of heparinase mix in 17 μL of 30 mM sodium acetate buffer, pH 7.0, containing 3 mM calcium acetate, at 37°C for 18 h. For keratanase digestion, the R-10G antigen was digested with 1.7 mU of keratanase in 20 μL of 25 mM Tris–HCl buffer, pH 7.4, at 37°C for 18 h. For keratanase II digestion, the R-10G antigen was digested with 0.5–10 mU of keratanase II in 20 μL of 10 mM sodium acetate buffer, pH 6.0, at 37°C for 18 h. For endo-β-galactosidase digestion, the R-10G antigen was digested with 2 mU of endo-β-galactosidase in 20 μL of 20 mM sodium acetate buffer, pH 5.8, at 37°C for 18 h. At the end of these digestions, the incubation mixtures were boiled for 3 min. For PNGase F digestion, Tic cell lysates or the R-10G antigen was heated in a solution consisting of 0.2% Nonidet P-40, 1% SDS, 50 mM 2-mercaptoethanol and 50 mM Tris–HCl buffer, pH 8.2, at 100°C for 5 min. An aliquot of the denatured proteins dissolved in a solution consisting of 0.15% Nonidet P-40, 3.6% octylglucoside, 2 mM EDTA, 63 mM Tris–HCl, pH 8.2 and 0.03% PMSF was digested with 2.0 U of PNGase F at 37°C for 18 h. For digestion with neuraminidase from *Arthrobacter ureafaciens*, the R-10G antigen was digested with 3.75 and 37.5 mU of the enzyme in 30 μL of 0.25 M sodium acetate buffer, pH 4.5, at 37°C for 18 h. For digestion with neuraminidase from *Vibrio cholerae* neuraminidase, the R-10G antigen was digested with 15 mU of the enzyme in 30 μL of 25 mM sodium acetate buffer, pH 5.5, containing 50% PIPA buffer, 77 mM NaCl, 4.5 mM $CaCl_2$ and 0.01% BSA, at 37°C for 18 h. For α1–3/4 fucosidase digestion, the R-10G antigen was digested with 15 μU of α1–3/4 fucosidase in 25 μL of 54 mM potassium phosphate buffer, pH 5.4, containing 0.15% Nonidet P-40, 480 mM $(NH_4)_2SO_4$ and 60 mM NaCl, at 37°C for 18 h. For α1–2 fucosidase digestion, the R-10G antigen was digested with 0.33 U or 2.0 U of α1–2 fucosidase in 10 μL of 50 mM sodium citrate buffer, pH 6.0, containing 0.2% Nonidet P-40, 100 mM NaCl and 0.01% BSA, at 37°C for 18 h.

Isolation of R-10G epitope glycopeptides from the R-10G antigen

The R-10G antigen (~14 μg protein derived from 3×10^7 Tic cells) was digested with pronase (1.4 μg) in 600 μL of 0.1 M borate buffer, pH 8.0, containing 10 mM calcium acetate and 0.04% NaN_3, at 37°C for 72 h. The digest was applied to a column of Sephadex 25 (1 × 17.5 cm), which had been equilibrated and eluted with 10 mM NH_4HCO_3, pH 8.0, to separate glycopeptides from small-size amino acids and peptides. The collected glycopeptides were applied to an R-10G-Sepharose 4B Column (gel volume; 0.4 mL), which had been equilibrated with 50 mM Tris–HCl buffer, pH 7.4, containing 150 mM NaCl. After washing the column with the equilibrium buffer, the glycopeptides bound to the column were eluted with 0.1 M diethylamine (pH 11.5) containing 150 mM NaCl. The eluate containing R-10G epitope glycopeptides was immediately neutralized by adding 1 M Tris–HCl buffer, pH 6.8. The passthrough fraction was collected as nonepitope glycopeptides and the bound fraction was collected as epitope glycopeptides.

Carbohydrate analyses of the R-10G antigen and the glycopeptides obtained therefrom

Neutral sugars were determined according to the procedures described previously (Terada et al. 2005). Briefly, samples were subjected to gas-phase hydrolysis in 4 N HCl and 4 N trifluoroacetic acid (50:50, v/v) 100°C for 4 h. The hydrolysates were reductively aminated with 2-aminopyridine (PA). Analysis of PA-monosaccharides was carried out essentially according to the method described by Suzuki et al. (1991). Sialic acid was determined according to the procedures described previously (Terada et al. 2005). Briefly, sialic acid was liberated from oligosaccharides by heating a sample in 0.1N H_2SO_4 at 80°C for 1.5 h and the liberated sialic acid was labeled with 1,2-diamino-4,5-methylenedioxybenzene (DMB) and quantitated by a fluorometric high-performance liquid chromatography (HPLC) method according to the method of Ito et al. (2002) on a C18 column. The amino sugars were determined according to the procedures described previously (Toyoda et al. 1998). Briefly, samples were subjected to hydrolysis in 6N HCl at 100°C for 2.5 h. Amino sugars released on hydrolysis were separated on a TSKgel

SCX column (4.6 mm i.d. × 150 mm) and eluted with 0.35 M borate/NaOH buffer (pH 7.6) at 60°C, high sensitivity being achieved by post-column reaction with 1% 2-cyanoacetamide. The oligosaccharides released from keratan sulfates on keratanase II digestion were separated with a reversed-phase ion-pair HPLC system using the fluorometric post-column detection, and the degree of sulfation was determined according to the previous procedures (Oguma et al. 2001) and a separate manuscript in preparation by Hirose et al. (in preparation).

Characterization of R-10G epitopes by means of ELISA

GAGs (10 mg/mL in 2-morpholinoethanesulfonic acid (MES) (Wako Pure Chemical Industries) buffer, pH 5.5) (1 mL) and the biotinylation reagent (50 mM EZ-link Hydrazide-Biotin (Pierce-Thermo Scientific) in dimethyl sulfoxide (DMSO) (Sigma-Aldrich)) (25 µL) were mixed, and then the condensing agent (100 mg/mL in MES buffer, pH 5.5, 1-ethyl-3-(3-dimethylaminopropyl) carbodimide-HCl (EDC), (Pierce-Thermo Scientific)) (12.5 µL) was added, followed by incubation overnight at room temperature. The biotinylated GAGs were dialyzed and stored at −20°C until needed for the ELISA assay. The streptavidin (20 µg/mL, Vector Laboratories, Burlingame, CA) (50 µL/well) was immobilized on an ELISA 96-well plate (Nalgene Nunc) overnight at 4°C. To the streptavidin-coated wells, the blocking solution (5-fold dilution, Applie Block, Seikagaku Biobusiness) (250 µL/well) was added, followed by incubation at room temperature for 2 h. After washing the wells with T-Tris-buffered saline (TBS) buffer (50 mM Tris–HCl, pH 7.5, 0.15%NaCl, 0.05% Tween 20 (Wako Pure Chemical Industries) and 0.1% ProCline 950 (Sigma-Aldrich)), the biotinylated GAGs (1 µg/mL, 100 µL) were added, followed by incubation for 30 min at room temperature. After washing the wells with T-TBS buffer, 100 µL of R-10G (1.0 µg/mL) or 5D4 (0.008 µg/mL) was added to the GAG-coated well, followed by incubation at room temperature for 1 h. After washing the wells with T-TBS buffer, the amounts of R-10G and 5D4 bound to the GAGs were determined by incubation with 100 µL of HRP-labeled second antibody (polyclonal goat anti-mouse immunoglobulins/HRP; Dako Cytomation) (0.5 µg/mL) and 100 µL of TMB (3,3′,5,5′-tetramethyl benzidine, BioFX). IgG1 from murine myeloma cells (1.0 µg/mL; Sigma-Aldrich) was used as a negative control. For inhibition experiments, increasing amounts of keratan sulfate (up to 1.0 µg/mL) isolated from bovine cornea or a high-sulfated keratan sulfate isolated from shark cartilage (Kerato polysulfate-1, (KPS-1)) (Furuhashi 1961) were added to the assay system composed of the biotinylated keratan sulfate from bovine cornea on a well plate and the assay was carried out as described above. For enzymatic modifications, the biotinylated keratan sulfate (20 µg/mL, 100 µL) was treated with keratanase (20 mU/mL, 100 µL) or keratanase II (20 mU/mL, 100 µL) at 37°C overnight, and the products were fixed to a streptavidin-coated well plate, and the binding activities of R-10G (1 µg/mL) and 5D4 (0.008 µg/mL) as to the residual oligosaccharide moieties on the biotinylated keratan sulfate were determined as described above.

All of the sugar residues have the D-configuration except fucose, which has the L-configuration.

Funding

This work was supported by Grants-in-Aid for Scientific Research B-20370052 (to T.K.), C-24570171 (to T.K.) and C-20590074 (to N.K.), for Young Scientists Start-up 20890255 (to M.N.), a Grant-in-Aid for the Japan Society for the Promotion of Science (JSPS) Fellows 22-9530 (to M.N.) from JSPS, a Grant-in-Aid for Scientific Research on Innovative Areas 24110517 (to T.K.) from the Ministry of Education, Culture, Sports, Science, and Technology of Japan, Grants from the Ministry of Health, Labor and Welfare of Japan (to M.K.F. and T.K.) and by the R-GIRO (Ritsumeikan Global Innovation Research Organization) Program (to H.T.).

Acknowledgements

We thank Tomoko Tominaga and Saori Kamo for the secretarial assistance.

Conflict of interest

M.K.F. is one of the patent holders and inventors of the basal medium: ESF. However, the licensing fee is <$10,000 dollars.

Abbreviations

BSA, bovine serum albumin; DAB, diaminobenzidine; DMB, 1,2-diamino-4,5-methylenedioxybenzene; DMSO, dimethyl sulfoxide; EC, embryonal carcinoma; ELISA, enzyme-linked immunosorbent assay; FAF, fatty acid-free; FBS, fetal bovine serum; FCA, Freund's complete adjuvant; Fuc, fucose; GAG, glycosaminoglycan; Gal, galactose; GalNAc, *N*-acetylgalactosamine, GCTM, germ cell tumor monoclonal; GlcNAc, *N*-acetylglucosamine; HAT, hypoxanthine, aminopterin and thymidine; hEC, human embryonal carcinoma; hES, human embryonic stem; hiPS, human induced pluripotent stem; HPLC, high performance liquid chromatography; HRP, horseradish peroxidase; iPS, induced pluripotent stem; KPS-1, kerato polysulfate-1; KS, keratan sulfate; LC, liquid chromatography; MEF, mouse embryonic fibroblast; MES, morpholinoethanesulfonic acid; MS, mass spectrometry; NIBIO, National Institute of Biomedical Innovation; PA, 2-aminopyridine; PAGE, polyacrylamide gel electrophoresis; PBS, phosphate-buffered saline; PFA, paraformaldehyde; PNGase F, peptide *N*-glycanase F; PODXL, SDS, sodium dodecyl sulfate; podocalyxin; SSEA, stage-specific embryonic antigen; TBS, Tris-buffered saline. TRA, tumor rejection antigen.

References

Adewumi O, Aflatoonian B, Ahrlund-Richter L, Amit M, Andrews PW, Beighton G, Bello PA, Benvenisty N, Berry LS, Bevan S, et al. 2007. Characterization of human embryonic stem cell lines by the International Stem Cell Initiative. *Nat Biotechnol.* 25:803–816.

Andrews PW, Banting G, Damjanov I, Arnaud D, Avner P. 1984. Three monoclonal antibodies defining distinct differentiation antigens associated with different high molecular weight polypeptides on the surface of human embryonal carcinoma cells. *Hybridoma.* 3:347–361.

Andrews PW, Marrink J, Hirka G, von Keitz A, Sleijfer DT, Gonczol E. 1991. The surface antigen phenotype of human embryonal carcinoma cells: Modulation upon differentiation and viral infection. *Recent Results Cancer Res.* 123:63–83.

Badcock G, Pigott C, Goepel J, Andrews PW. 1999. The human embryonal carcinoma marker antigen TRA-1–60 is a sialylated keratan sulfate proteoglycan. *Cancer Res.* 59:4715–4719.

Brandenberger R, Wei H, Zhang S, Lei S, Murage J, Fisk GJ, Li Y, Xu C, Fang R, Guegler K, et al. 2004. Transcriptome characterization elucidates signaling networks that control human ES cell growth and differentiation. *Nat Biotechnol.* 22:707–716.

Brown GM, Nieduszynski IA, Morris HG, Abram BL, Huckerby TN, Block JA. 1995. Skeletal keratan sulphate structural analysis using keratanase II digestion followed by high-performance anion-exchange chromatography. *Glycobiology.* 5:311–317.

Cai J, Chen J, Liu Y, Miura T, Luo Y, Loring JF, Freed WJ, Rao MS, Zeng X. 2006. Assessing self-renewal and differentiation in human embryonic stem cell lines. *Stem Cells.* 24:516–530.

Cooper S, Pera MF, Bennett W, Finch JT. 1992. A novel keratan sulphate proteoglycan from a human embryonal carcinoma cell line. *Biochem J.* 286(Pt 3):959–966.

Fukuda MN, Matsumura G. 1976. Endo-beta-galactosidase of Escherichia freundii. Purification and endoglycosidic action on keratan sulfates, oligosaccharides, and blood group active glycoprotein. *J Biol Chem.* 251:6218–6225.

Furue M, Okamoto T, Hayashi Y, Okochi H, Fujimoto M, Myoishi Y, Abe T, Ohnuma K, Sato GH, Asashima M, et al. 2005. Leukemia inhibitory factor as an anti-apoptotic mitogen for pluripotent mouse embryonic stem cells in a serum-free medium without feeder cells. *In Vitro Cell Dev Biol Anim.* 41:19–28.

Furue MK, Na J, Jackson JP, Okamoto T, Jones M, Baker D, Hata R, Moore HD, Sato JD, Andrews PW. 2008. Heparin promotes the growth of human embryonic stem cells in a defined serum-free medium. *Proc Natl Acad Sci USA.* 105:13409–13414.

Furuhashi T. 1961. Polysulfated mucopolysaccharides of elasmobranch cartilage. *J Biochem.* 50:546–547.

Hirose Y, Kinoshita-Toyoda A, Toyoda H. Microdetermination of keratan sulfate in biological samples by high-performance liquid chromatography with postcolumn fluorometric detection. in preparation.

Ito M, Hirabayashi Y, Yamagata T. 1986. Substrate specificity of endo-beta-galactosidases from Flavobacterium keratolyticus and Escherichia freundii is different from that of Pseudomonas sp. *J Biochem.* 100:773–780.

Ito M, Ikeda K, Suzuki Y, Tanaka K, Saito M. 2002. An improved fluorometric high-performance liquid chromatography method for sialic acid determination: An internal standard method and its application to sialic acid analysis of human apolipoprotein E. *Anal Biochem.* 300:260–266.

Kannagi R, Cochran NA, Ishigami F, Hakomori S, Andrews PW, Knowles BB, Solter D. 1983. Stage-specific embryonic antigens (SSEA-3 and -4) are epitopes of a unique globo-series ganglioside isolated from human teratocarcinoma cells. *EMBO J.* 2:2355–2361.

Kannagi R, Levery SB, Ishigami F, Hakomori S, Shevinsky LH, Knowles BB, Solter D. 1983. New globoseries glycosphingolipids in human teratocarcinoma reactive with the monoclonal antibody directed to a developmentally regulated antigen, stage-specific embryonic antigen 3. *J Biol Chem.* 258:8934–8942.

Kerjaschki D, Sharkey DJ, Farquhar MG. 1984. Identification and characterization of podocalyxin—the major sialoprotein of the renal glomerular epithelial cell. *J Cell Biol.* 98:1591–1596.

Kershaw DB, Beck SG, Wharram BL, Wiggins JE, Goyal M, Thomas PE, Wiggins RC. 1997. Molecular cloning and characterization of human podocalyxin-like protein. Orthologous relationship to rabbit PCLP1 and rat podocalyxin. *J Biol Chem.* 272:15708–15714.

Kershaw DB, Wiggins JE, Wharram BL, Wiggins RC. 1997. Assignment of the human podocalyxin-like protein (PODXL) gene to 7q32-q33. *Genomics.* 45:239–240.

Laemmli UK. 1970. Cleavage of structural proteins during the assembly of the head of bacteriophage T4. *Nature.* 227:680–685.

Mehmet H, Scudder P, Tang PW, Hounsell EF, Caterson B, Feizi T. 1986. The antigenic determinants recognized by three monoclonal antibodies to keratan sulphate involve sulphated hepta- or larger oligosaccharides of the poly(N-acetyllactosamine) series. *Eur J Biochem.* 157:385–391.

Natunen S, Satomaa T, Pitkanen V, Salo H, Mikkola M, Natunen J, Otonkoski T, Valmu L. 2011. The binding specificity of the marker antibodies Tra-1–60 and Tra-1–81 reveals a novel pluripotency-associated type 1 lactosamine epitope. *Glycobiology.* 21:1125–1130.

Nielsen JS, McNagny KM. 2009. The role of podocalyxin in health and disease. *J Am Soc Nephrol.* 20:1669–1676.

Oguma T, Toyoda H, Toida T, Imanari T. 2001. Analytical method for keratan sulfates by high-performance liquid chromatography/turbo-ionspray tandem mass spectrometry. *Anal Biochem.* 290:68–73.

Pera MF, Blasco-Lafita MJ, Cooper S, Mason M, Mills J, Monaghan P. 1988. Analysis of cell-differentiation lineage in human teratomas using new monoclonal antibodies to cytostructural antigens of embryonal carcinoma cells. *Differentiation.* 39:139–149.

Sassetti C, Tangemann K, Singer MS, Kershaw DB, Rosen SD. 1998. Identification of podocalyxin-like protein as a high endothelial venule ligand for L-selectin: Parallels to CD34. *J Exp Med.* 187:1965–1975.

Sassetti C, Van Zante A, Rosen SD. 2000. Identification of endoglycan, a member of the CD34/podocalyxin family of sialomucins. *J Biol Chem.* 275:9001–9010.

Schopperle WM, DeWolf WC. 2007. The TRA-1-60 and TRA-1-81 human pluripotent stem cell markers are expressed on podocalyxin in embryonal carcinoma. *Stem Cells.* 25:723–730.

Shevinsky LH, Knowles BB, Damjanov I, Solter D. 1982. Monoclonal antibody to murine embryos defines a stage-specific embryonic antigen expressed on mouse embryos and human teratocarcinoma cells. *Cell.* 30:697–705.

Sulak O, Cioci G, Delia M, Lahmann M, Varrot A, Imberty A, Wimmerova M. 2010. A TNF-like trimeric lectin domain from *Burkholderia cenocepacia* with specificity for fucosylated human histo-blood group antigens. *Structure.* 18:59–72.

Suzuki J, Kondo A, Kato I, Hase S, Ikenaka T. 1991. Analysis by high-performance anion-exchange chromatography of component sugars as their fluorescent pyridylamino derivatives(analytical chemistry). *Agric Biol Chem.* 55:283–284.

Takahashi K, Tanabe K, Ohnuki M, Narita M, Ichisaka T, Tomoda K, Yamanaka S. 2007. Induction of pluripotent stem cells from adult human fibroblasts by defined factors. *Cell.* 131:861–872.

Tang C, Lee AS, Volkmer JP, Sahoo D, Nag D, Mosley AR, Inlay MA, Ardehali R, Chavez SL, Pera RR, et al. 2011. An antibody against SSEA-5 glycan on human pluripotent stem cells enables removal of teratoma-forming cells. *Nat Biotechnol.* 29:829–834.

Tateno H, Toyota M, Saito S, Onuma Y, Ito Y, Hiemori K, Fukumura M, Matsushima A, Nakanishi M, Ohnuma K, et al. 2011. Glycome diagnosis of human induced pluripotent stem cells using lectin microarray. *J Biol Chem.* 286:20345–20353.

Terada M, Khoo KH, Inoue R, Chen CI, Yamada K, Sakaguchi H, Kadowaki N, Ma BY, Oka S, Kawasaki T, et al. 2005. Characterization of oligosaccharide ligands expressed on SW1116 cells recognized by mannan-binding protein. A highly fucosylated polylactosamine type *N*-glycan. *J Biol Chem.* 280:10897–10913.

Towbin H, Staehelin T, Gordon J. 1992. Electrophoretic transfer of proteins from polyacrylamide gels to nitrocellulose sheets: Procedure and some applications. 1979. *Biotechnology.* 24:145–149.

Toyoda H, Demachi Y, Komoriya S, Furuya N, Toida T, Imanari T. 1998. Characterization and determination of human urinary keratan sulfate. *Chem Pharm Bull (Tokyo).* 46:97.

Toyoda M, Yamazaki-Inoue M, Itakura Y, Kuno A, Ogawa T, Yamada M, Akutsu H, Takahashi Y, Kanzaki S, Narimatsu H, et al. 2011. Lectin microarray analysis of pluripotent and multipotent stem cells. *Genes Cells.* 16:1–11.

Watanabe K, Ueno M, Kamiya D, Nishiyama A, Matsumura M, Wataya T, Takahashi JB, Nishikawa S, Nishikawa S, Muguruma K, et al. 2007. A ROCK inhibitor permits survival of dissociated human embryonic stem cells. *Nat Biotechnol.* 25:681–686.

Wright AJ, Andrews PW. 2009. Surface marker antigens in the characterization of human embryonic stem cells. *Stem Cell Research.* 3:3–11.

Efficient Generation of Functional Hepatocytes From Human Embryonic Stem Cells and Induced Pluripotent Stem Cells by HNF4α Transduction

Kazuo Takayama[1,2], Mitsuru Inamura[1,2], Kenji Kawabata[2,3], Kazufumi Katayama[1], Maiko Higuchi[2], Katsuhisa Tashiro[2], Aki Nonaka[2], Fuminori Sakurai[1], Takao Hayakawa[4,5], Miho Kusuda Furue[6,7] and Hiroyuki Mizuguchi[1,2,8]

[1]Laboratory of Biochemistry and Molecular Biology, Graduate School of Pharmaceutical Sciences, Osaka University, Osaka, Japan; [2]Laboratory of Stem Cell Regulation, National Institute of Biomedical Innovation, Osaka, Japan; [3]Laboratory of Biomedical Innovation, Graduate School of Pharmaceutical Sciences, Osaka University, Osaka, Japan; [4]Pharmaceutics and Medical Devices Agency, Tokyo, Japan; [5]Pharmaceutical Research and Technology Institute, Kinki University, Osaka, Japan; [6]JCRB Cell Bank, Division of Bioresources, National Institute of Biomedical Innovation, Osaka, Japan; [7]Laboratory of Cell Processing, Institute for Frontier Medical Sciences, Kyoto University, Kyoto, Japan; [8]The Center for Advanced Medical Engineering and Informatics, Osaka University, Osaka, Japan

Hepatocyte-like cells from human embryonic stem cells (ESCs) and induced pluripotent stem cells (iPSCs) are expected to be a useful source of cells drug discovery. Although we recently reported that hepatic commitment is promoted by transduction of SOX17 and HEX into human ESC- and iPSC-derived cells, these hepatocyte-like cells were not sufficiently mature for drug screening. To promote hepatic maturation, we utilized transduction of the hepatocyte nuclear factor 4α (HNF4α) gene, which is known as a master regulator of liver-specific gene expression. Adenovirus vector-mediated overexpression of HNF4α in hepatoblasts induced by SOX17 and HEX transduction led to upregulation of epithelial and mature hepatic markers such as cytochrome P450 (CYP) enzymes, and promoted hepatic maturation by activating the mesenchymal-to-epithelial transition (MET). Thus HNF4α might play an important role in the hepatic differentiation from human ESC-derived hepatoblasts by activating the MET. Furthermore, the hepatocyte like-cells could catalyze the toxication of several compounds. Our method would be a valuable tool for the efficient generation of functional hepatocytes derived from human ESCs and iPSCs, and the hepatocyte-like cells could be used for predicting drug toxicity.

Received 19 July 2011; accepted 28 September 2011; published online 8 November 2011. doi:10.1038/mt.2011.234

INTRODUCTION

Human embryonic stem cells (ESCs) and induced pluripotent stem cells (iPSCs) are able to replicate indefinitely and differentiate into most of the body's cell types.[1,2] They could provide an unlimited source of cells for various applications. Hepatocyte-like cells, which are differentiated from human ESCs and iPSCs, would be useful for basic research, regenerative medicine, and drug discovery.[3] In particular, it is expected that hepatocyte-like cells will be utilized as a tool for cytotoxicity screening in the early phase of pharmaceutical development. To catalyze the toxication of several compounds, hepatocyte-like cells need to be mature enough to exhibit hepatic functions, including high activity levels of the cytochrome P450 (CYP) enzymes. Because the present technology for the generation of hepatocyte-like cells from human ESCs and iPSCs, which is expected to be utilized for drug discovery, is not refined enough for this application, it is necessary to improve the efficiency of hepatic differentiation. Although conventional methods such as growth factor-mediated hepatic differentiation are useful to recapitulate liver development, they lead to only a heterogeneous hepatocyte population.[4–6] Recently, we showed that transcription factors are transiently transduced to promote hepatic differentiation in addition to the conventional differentiation method which uses only growth factors.[7] Ectopic expression of Sry-related HMG box 17 (SOX17) or hematopoietically expressed homeobox (HEX) by adenovirus (Ad) vectors in human ESC-derived mesendoderm or definitive endoderm (DE) cells markedly enhances the endoderm differentiation or hepatic commitment, respectively.[7,8] However, further hepatic maturation is required for drug screening.

The transcription factor hepatocyte nuclear factor 4α (HNF4α) is initially expressed in the developing hepatic diverticulum on E8.75,[9,10] and its expression is elevated as the liver develops. A previous loss-of-function study showed that HNF4α plays a critical role in liver development; conditional deletion of *HNF4α* in fetal hepatocytes results in the faint expression of many mature hepatic enzymes and the impairment of normal liver morphology.[11] The genome-scale chromatin immunoprecipitation assay showed that HNF4α binds to the promoters of nearly half of the genes expressed in the mouse liver,[12] including cell adhesion and junctional proteins,[13] which are important in

Correspondence: Hiroyuki Mizuguchi, Laboratory of Biochemistry and Molecular Biology, Graduate School of Pharmaceutical Sciences, Osaka University, 1-6 Yamadaoka, Suita, Osaka 565-0871, Japan. E-mail: mizuguch@phs.osaka-u.ac.jp

the hepatocyte epithelial structure.[14] In addition, HNF4α plays a critical role in hepatic differentiation and in a wide variety of liver functions, including lipid and glucose metabolism.[15,16] Although HNF4α could promote transdifferentiation into hepatic lineage from hematopoietic cells,[17] the function of HNF4α in hepatic differentiation from human ESCs and iPSCs remains unknown. A previous study showed that hepatic differentiation from mouse hepatic progenitor cells is promoted by HNF4α, although many of the hepatic markers that they examined were target genes of HNF4α.[18] They transplanted the HNF4α-overexpressed mouse hepatic progenitor cells to promote hepatic differentiation, but they did not examine the markers that relate to hepatic maturation such as CYP enzymes, conjugating enzymes, and hepatic transporters.

In this study, we examined the role of HNF4α in hepatic differentiation from human ESCs and iPSCs. The human ESC- and iPSC-derived hepatoblasts, which were efficiently generated by sequential transduction of SOX17 and HEX, were transduced with HNF4α-expressing Ad vector (Ad-HNF4α), and then the expression of hepatic markers of the hepatocyte-like cells were assessed. In addition, we examined whether or not the hepatocyte-like cells, which were generated by sequential transduction of SOX17, HEX, and HNF4α, were able to predict the toxicity of several compounds.

RESULTS

Stage-specific HNF4α transduction in hepatoblasts selectively promotes hepatic differentiation

The transcription factor HNF4α plays an important role in both liver generation[11] and hepatic differentiation from human ESCs and iPSCs (**Supplementary Figure S1**). We expected that hepatic differentiation could be accelerated by HNF4α transduction. To examine the effect of forced expression of HNF4α in the hepatic differentiation from human ESC- and iPSC-derived cells, we used a fiber-modified Ad vector.[19] Initially, we optimized the time period for Ad-HNF4α transduction. Human ESC (H9)-derived DE cells (day 6) (**Supplementary Figures S2** and **S3a**), hepatoblasts (day 9) (**Supplementary Figures S2** and **S3b**), or a heterogeneous population consisting of hepatoblasts, hepatocytes, and cholangiocytes (day 12) (**Supplementary Figures S2** and **S3c**) were transduced with Ad-HNF4α and then the Ad-HNF4α-transduced cells were cultured until day 20 of differentiation (Figure 1). We ascertained the expression of exogenous *HNF4α* in human ESC-derived hepatoblasts (day 9) transduced with Ad-HNF4α (**Supplementary Figure S4**). The transduction of Ad-HNF4α into human ESC-derived hepatoblasts (day 9) led to the highest expression levels of the hepatocyte markers *albumin* (*ALB*)[20] and *α-1-antitrypsin* (Figure 1a). In contrast, the expression levels of the cholangiocyte markers *cytokeratin 7* (*CK7*)[21] and *SOX9*[22] were

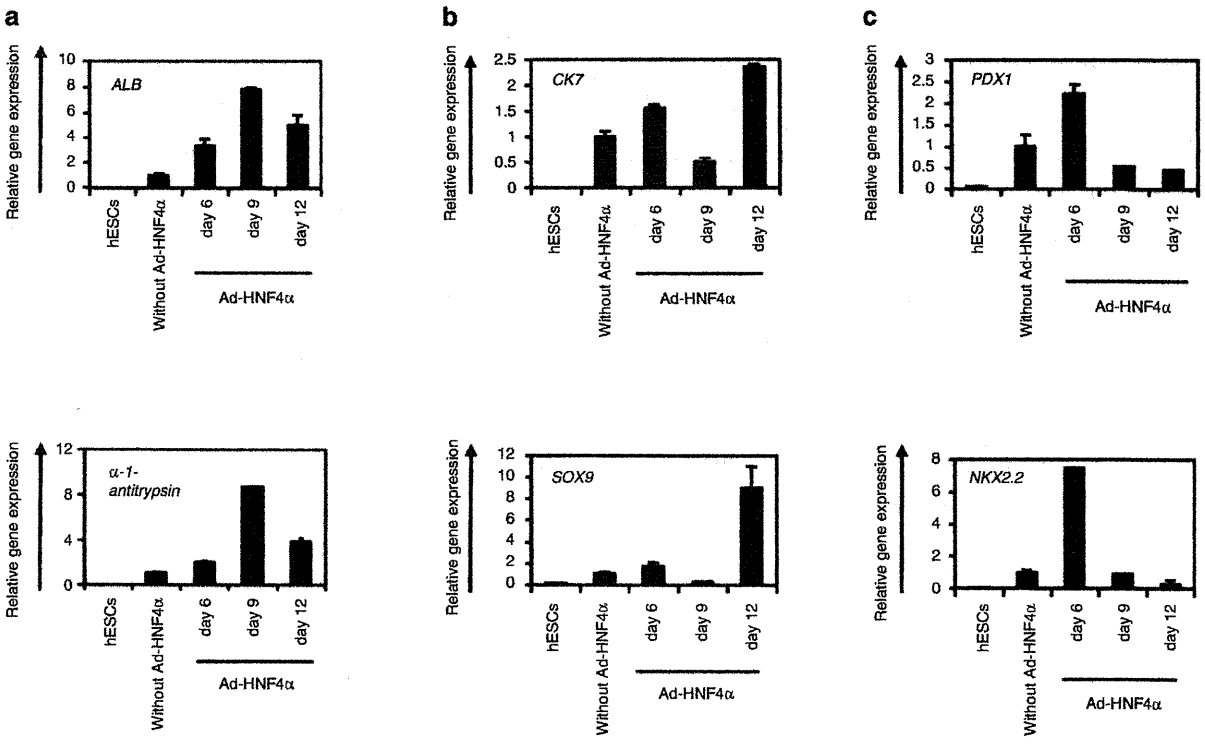

Figure 1 Transduction of HNF4α into hepatoblasts promotes hepatic differentiation. (**a–c**) The human ESC (H9)-derived cells, which were cultured for 6, 9, or 12 days according to the protocol described in **Figure 2a**, were transduced with 3,000 vector particles (VP)/cell of Ad-HNF4α for 1.5 hours and cultured until day 20. The gene expression levels of (**a**) hepatocyte markers (*ALB* and *α-1-antitrypsin*), (**b**) cholangiocyte markers (*CK7* and *SOX9*), and (**c**) pancreas markers (*PDX1* and *NKX2.2*) were examined by real-time RT-PCR on day 0 (human ESCs (hESCs)) or day 20 of differentiation. The horizontal axis represents the days when the cells were transduced with Ad-HNF4α. On the y-axis, the level of the cells without Ad-HNF4α transduction on day 20 was taken as 1.0. All data are represented as means ± SD ($n = 3$). ESC, embryonic stem cell; HNF4α, hepatocyte nuclear factor 4α; RT-PCR, reverse transcription-PCR.

downregulated in the cells transduced on day 9 as compared with nontransduced cells (Figure 1b). This might be because hepatic differentiation was selectively promoted and biliary differentiation was repressed by the transduction of HNF4α in hepatoblasts. The expression levels of the pancreas markers *PDX1*[23] and *NKX2.2*[24] did not make any change in the cells transduced on day 9 as compared with nontransduced cells (Figure 1c). Interestingly, the expression levels of the pancreas markers were upregulated, when Ad-HNF4α transduction was performed into DE cells (day 6) (Figure 1c). These results suggest that HNF4α might promote not only hepatic differentiation but also pancreatic differentiation, although the optimal stage of HNF4 transduction for the differentiation of each cell is different. We have confirmed that there was no difference between nontransduced cells and Ad-LacZ-transduced cells in the gene expression levels of all the markers investigated in Figure 1a–c (data not shown). We also confirmed that Ad vector-mediated gene expression in the human ESC-derived hepatoblasts (day 9) continued until day 14 and almost disappeared on day 18 (**Supplementary Figure S5**). These results indicated that the stage-specific HNF4α overexpression in human ESC-derived hepatoblasts (day 9) was essential for promoting efficient hepatic differentiation.

Transduction of HNF4α into human ESC- and iPSC-derived hepatoblasts efficiently promotes hepatic maturation

From the results of Figure 1, we decided to transduce hepatoblasts (day 9) with Ad-HNF4α. To determine whether hepatic maturation is promoted by Ad-HNF4α transduction, Ad-HNF4α-transduced cells were cultured until day 20 of differentiation according to the schematic protocol described in Figure 2a. After the hepatic maturation, the morphology of human ESCs was gradually changed into that of hepatocytes: polygonal with distinct round nuclei (day 20) (Figure 2b). Interestingly, a portion of the hepatocyte-like cells, which were ALB[20]-, CK18[21]-, CYP2D6-, and CYP3A4[25]-positive cells, had double nuclei, which was also observed in primary human hepatocytes (Figure 2b,c, and **Supplementary Figure S6**). We also examined the hepatic gene expression levels on day 20 of differentiation (Figure 3a,b). The gene expression analysis of *CYP1A2*, *CYP2C9*, *CYP2C19*, *CYP2D6*, *CYP3A4*, and *CYP7A1*[25] showed higher expression levels in all of Ad-SOX17-, Ad-HEX-, and Ad-HNF4α-transduced cells (three factors-transduced cells) as compared with those in both Ad-SOX17- and Ad-HEX-transduced cells (two factors-transduced cells) on day 20 (Figure 3a). The gene expression level of NADPH-CYP reductase

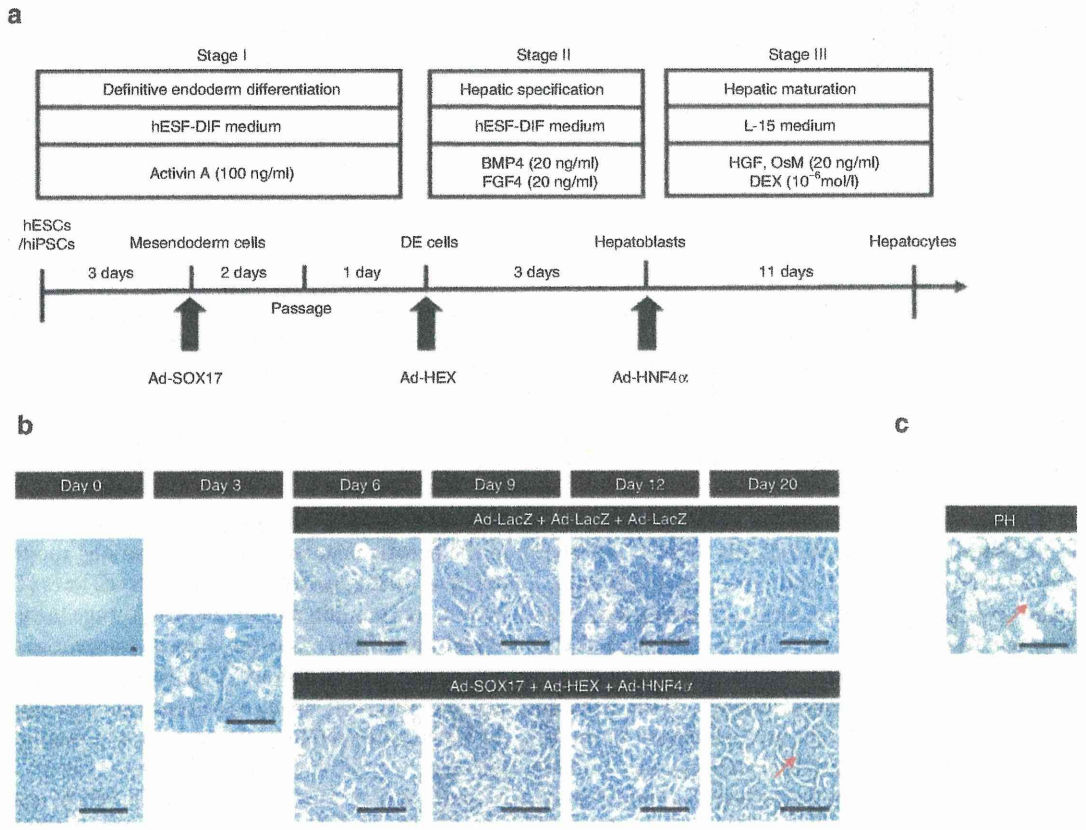

Figure 2 Hepatic differentiation of human ESCs and iPSCs transduced with three factors. (**a**) The procedure for differentiation of human ESCs and iPSCs into hepatocytes via DE cells and hepatoblasts is presented schematically. The hESF-DIF medium was supplemented with 10 μg/ml human recombinant insulin, 5 μg/ml human apotransferrin, 10 μmol/l 2-mercaptoethanol, 10 μmol/l ethanolamine, 10 μmol/l sodium selenite, and 0.5 mg/ml fatty-acid-free BSA. The L15 medium was supplemented with 8.3% tryptose phosphate broth, 8.3% FBS, 10 μmol/l hydrocortisone 21-hemisuccinate, 1 μmol/l insulin, and 25 mmol/l $NaHCO_3$. (**b**) Sequential morphological changes (day 0–20) of human ESCs (H9) differentiated into hepatocytes via DE cells and hepatoblasts are shown. Red arrow shows the cells that have double nuclei. (**c**) The morphology of primary human hepatocytes is shown. Bar represents 50 μm. BSA, bovine serum albumin; DE, definitive endoderm; ESC, embryonic stem cell; iPSC, induced pluripotent stem cell.

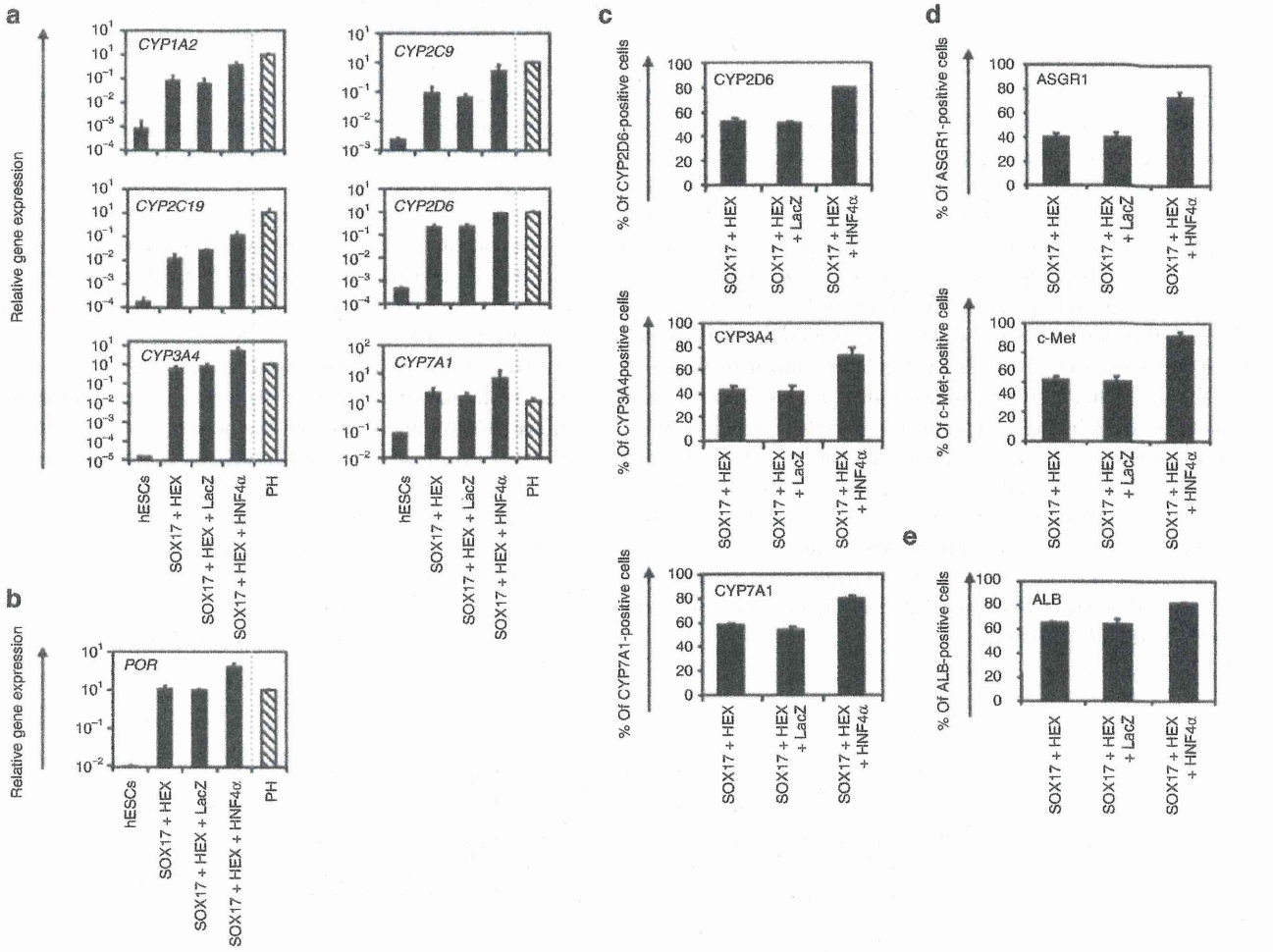

Figure 3 Transduction of HNF4α promotes hepatic maturation from human ESCs and iPSCs. (**a**,**b**) The human ESCs were differentiated into hepatocytes according to the protocol described in **Figure 2a**. On day 20 of differentiation, the gene expression levels of (**a**) CYP enzymes (*CYP1A2*, *CYP2C9*, *CYP2C19*, *CYP2D6*, *CYP3A4*, and *CYP7A1*) and (**b**) *POR* were examined by real-time RT-PCR in undifferentiated human ESCs (hESCs), the hepatocyte-like cells, and primary human hepatocytes (PH, hatched bar). On the y-axis, the expression level of primary human hepatocytes, which were cultured for 48 hours after the cells were plated, was taken as 1.0. (**c**–**e**) The hepatocyte-like cells (day 20) were subjected to immunostaining with (**c**) anti-drug-metabolizing enzymes (CYP2D6, CYP3A4, and CYP7A1), (**d**) anti-hepatic surface protein (ASGR1 and c-Met), and (**e**) anti-ALB antibodies, and then the percentage of antigen-positive cells was examined by flow cytometry on day 20 of differentiation. All data are represented as means ± SD (n = 3). ESC, embryonic stem cell; HNF4α, hepatocyte nuclear factor 4α; iPSC, induced pluripotent stem cell.

(POR)[26], which is required for the normal function of CYPs, was also higher in the three factors-transduced cells (**Figure 3b**). The gene expression analysis of ALB, α-1-antitrypsin (α-1-AT), transthyretin, hepatic conjugating enzymes, hepatic transporters, and hepatic transcription factors also showed higher expression levels in the three factors-transduced cells (**Supplementary Figures S7** and **S8**). Moreover, the gene expression levels of these hepatic markers of three factor-transduced cells were similar to those of primary human hepatocytes, although the levels depended on the type of gene (**Figure 3a,b**, and **Supplementary Figures S7** and **S8**). To confirm that similar results could be obtained with human iPSCs, we used three human iPS cell lines (201B7, Dotcom, and Tic). The gene expression of hepatic markers in human ESC- and iPSC-derived hepatocytes were analyzed by real-time reverse transcription-PCR on day 20 of differentiation. Three human iPS cell lines as well as human ESCs also effectively differentiated into hepatocytes in response to transduction of the three factors (**Supplementary Figure S9**). Interestingly, we observed differences in the hepatic maturation efficiency among the three human iPS cell lines. That is, two of the human iPS cell lines (Tic and Dotcom) were more committed to the hepatic lineage than another human iPS cell line (201B7). Because almost homogeneous hepatocyte-like cells would be more useful in basic research, regenerative medicine, and drug discovery, we also examined whether our novel methods for hepatic maturation could generate a homogeneous hepatocyte population by flow cytometry analysis (**Figure 3c–e**). The percentages of CYP2D6-, CYP3A4-, and CYP7A1-positive cells were ~80% in the three factors-transduced cells, while they were ~50% in the two factors-transduced cells (**Figure 3c**). The percentages of hepatic surface antigen (asialoglycoprotein receptor 1 (ASGR1] and met proto-oncogene (c-Met))-positive cells (**Figure 3d**) and ALB-positive cells (**Figure 3e**) were also ~80% in the three factors-transduced cells. These results indicated that a nearly homogeneous population was obtained by our differentiation protocol

using the transduction of three functional genes (SOX17, HEX, and HNF4α).

The three factors-transduced cells have characteristics of functional hepatocytes

The hepatic functions of the hepatocyte-like cells, such as the uptake of low-density lipoprotein (LDL) and CYP enzymes activity, of the hepatocyte-like cells were examined on day 20 of differentiation. Approximately 87% of the three factors-transduced cells uptook LDL in the medium, whereas only 44% of the two factors-transduced cells did so (**Figure 4a**). The activities of CYP enzymes of the hepatocyte-like cells were measured according to the metabolism of the CYP3A4, CYP2C9, or CYP1A2 substrates (**Figure 4b**). The metabolites were detected in the three factors-transduced cells and their activities were higher than those of the two factors-transduced cells (dimethyl sulfoxide (DMSO) column). We further tested the induction of CYP3A4, CYP2C9, and CYP1A2 by chemical stimulation, since CYP3A4, CYP2C9, and CYP1A2 are the important prevalent CYP isozymes in the liver and are involved in the metabolism of a significant proportion of the currently available commercial drugs (rifampicin or omeprazole column). It is well known that CYP3A4 and CYP2C9 can be induced by rifampicin, whereas CYP1A2 can be induced by omeprazole. The hepatocyte-like cells were treated with either of these. Although undifferentiated human ESCs responsed to neither rifampicin nor omeprazole (data not shown), the hepatocyte-like cells produced more metabolites in response to chemical stimulation as well as primary hepatocytes (**Figure 4b**). The activity levels of the hepatocyte-like cells as compared with those of primary human hepatocytes depended on the types of CYP; the CYP3A4 activity of the hepatocyte-like cells was similar to that of primary human hepatocytes, whereas the CYP2C9 and CYP1A2 activities of the hepatocyte-like cells were slightly lower than those of primary human hepatocytes (**Figure 3a**). These results indicated that high levels of functional CYP enzymes were detectable in the hepatocyte-like cells.

The metabolism of diverse compounds involving uptake, conjugation, and the subsequent release of the compounds is an important function of hepatocytes. Uptake and release of Indocyanine green (ICG) can often be used to identify hepatocytes in ESC differentiation models.[27] To investigate this function in our hepatocyte-like cells, we compared this ability of the three factors-transduced cells with that of the two factors-transduced cells on day 20 of differentiation (**Figure 4c**). The three factors-transduced cells had more ability to uptake ICG and to excrete ICG by culturing without ICG for 6 hours. We also examined whether the hepatocyte-like cells could store glycogen, a characteristic of functional hepatocytes (**Figure 4d**). On day 20 of differentiation, the three factors-transduced cells and the two factors-transduced cells were stained for cytoplasmic glycogen using the Periodic Acid-Schiff staining procedure. The three factors-transduced cells exhibited more abundant storage of glycogen than the two-factors-transduced cells. These results showed that abundant hepatic functions, such as uptake and excretion of ICG and storage of glycogen, were obtained by the transduction of three factors.

Many adverse drug reactions are caused by the CYP-dependent activation of drugs into reactive metabolites.[28] In order to examine metabolism-mediated toxicity and to improve the safety of drug candidates, primary human hepatocytes are widely used.[28] Because primary human hepatocytes have quite different characteristics among distinct lots and because it is difficult to purchase large amounts of primary human hepatocytes that have the same characteristics, hepatocyte-like cells are expected to be used for this purpose. To examine whether our hepatocyte-like cells could be used to predict metabolism-mediated toxicity, the hepatocyte-like cells were incubated with four substrates (troglitazone, acetaminophen, cyclophosphamide, and carbamazepine), which are known to generate toxic metabolites by CYP enzymes, and then the cell viability was measured (**Figure 4e**). The cell viability of the two factors plus Ad-LacZ-tansduced cells were higher than that of the three factors-transduced cells at each different concentration of four test compounds. These results indicated that the three factors-transduced cells could more efficiently metabolize the test compounds and thereby induce higher toxicity than either the two factors-transduced cells or undifferentiated human ESCs. The cell viability of the three factors-transduced cells was slightly higher than that of primary human hepatocytes.

HNF4α promotes hepatic maturation by activating mesenchymal-to-epithelial transition

HNF4α is known as a dominant regulator of the epithelial phenotype because its ectopic expression in fibroblasts (such as NIH 3T3 cells) induces mesenchymal-to-epithelial transition (MET)[11], although it is not known whether HNF4α can promote MET in hepatic differentiation. Therefore, we examined whether HNF4α transduction promotes hepatic maturation from hepatoblasts by activating MET. To clarify whether MET is activated by HNF4α transduction, the human ESC-derived hepatoblasts (day 9) were transduced with Ad-LacZ or Ad-HNF4α, and the resulting phenotype was analyzed on day 12 of differentiation (**Figure 5**). This time, we confirmed that HNF4α transduction decreased the population of N-cadherin (hepatoblast marker)-positive cells,[29] whereas it increased that of ALB (hepatocyte marker)-positive cells (**Figure 5a**). The number of CK7 (cholangiocyte marker)-positive population did not change (**Figure 5a**). To investigate whether these results were attributable to MET, the alteration of the expression of several mesenchymal and epithelial markers was examined (**Figure 5b**). The human ESC-derived hepatoblasts (day 9) were almost homogeneously N-cadherin[30] (mesenchymal marker)-positive and E-cadherin[11] (epithelial marker)-negative, demonstrating that human ESC-derived hepatoblasts have mesenchymal characteristics (**Figure 5a,b**). After HNF4α transduction, the number of E-cadherin-positive cells was increased and reached ~90% on day 20, whereas that of N-cadherin-positive cells was decreased and was less than 5% on day 20 (**Supplementary Figure S10**). These results indicated that MET was promoted by HNF4α transduction in hepatic differentiation from hepatoblasts. Interestingly, the number of growing cells was decreased by HNF4α transduction (**Figure 5c**), and the cell growth was delayed by HNF4α transduction (**Supplementary Figure S11**). This decrease in the number of growing cells might have been because the differentiation was promoted by HNF4α transduction. We also confirmed that MET was promoted by HNF4α transduction in the gene expression levels (**Figure 5d**).

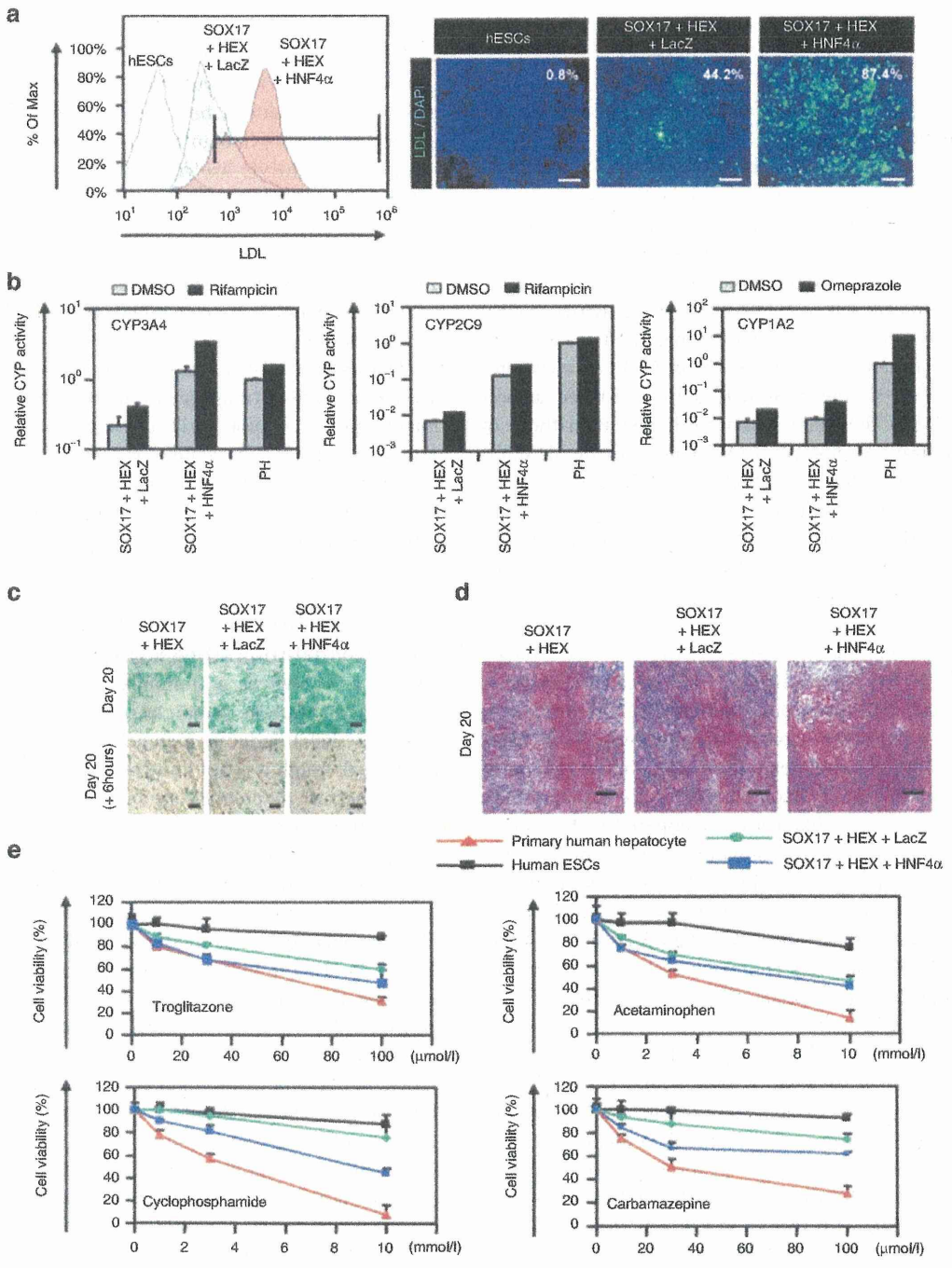

Figure 4 Transduction of the three factors enhances hepatic functions. The human ESCs were differentiated into hepatoblasts and transduced with 3,000 VP/cell of Ad-LacZ or Ad-HNF4α for 1.5 hours and cultured until day 20 of differentiation according to the protocol described in **Figure 2a**. The hepatic functions of the two factors plus Ad-LacZ-transduced cells (SOX17+HEX+LacZ) and the three factors-transduced cells (SOX17+HEX+HNF4α) were compared. (**a**) Undifferentiated human ESCs (hESCs) and the hepatocyte-like cells (day 20) were cultured with medium containing Alexa-Flour 488-labeled LDL (green) for 1 hour, and immunohistochemistry and flow cytometry analysis were performed. The percentage of LDL-positive cells was measured by flow cytometry. Nuclei were counterstained with DAPI (blue). The bar represents 100 μm. (**b**) Induction of CYP3A4 (left), CYP2C9 (middle), or CYP1A2 (right) by DMSO (gray bar), rifampicin (black bar), or omeprazole (black bar) in the hepatocyte-like cells (day 20) and primary human hepatocytes (PH), which were cultured for 48 hours after the cells were plated. On the y-axis, the activity of primary human hepatocytes that have been cultured with medium containing DMSO was taken as 1.0. (**c**) The hepatocyte-like cells (day 20) (upper column) were examined for their ability to take up Indocyanin Green (ICG) and release it 6 hours thereafter (lower column). (**d**) Glycogen storage of the hepatocyte-like cells (day 20) was assessed by Periodic Acid-Schiff (PAS) staining. PAS staining was performed on day 20 of differentiation. Glycogen storage is indicated by pink or dark red-purple cytoplasms. The bar represents 100 μm. (**e**) The cell viability of undifferentiated human ESCs (black), two factors plus Ad-LacZ-tansduced cells (green), the three factors-transduced cells (blue), and primary human hepatocytes (red) was assessed by Alamar Blue assay after 48 hours exposure to different concentrations of four test compounds (troglitazone, acetaminophen, cyclophosphamide, and carbamazepine). The cell viability is expressed as a percentage of cells treated with solvent only treat: 0.1% DMSO except for carbamazepine: 0.5% DMSO. All data are represented as means ± SD ($n = 3$). ESC, embryonic stem cell; DMSO, dimethyl sulfoxide; LDL, low-density lipoprotein.

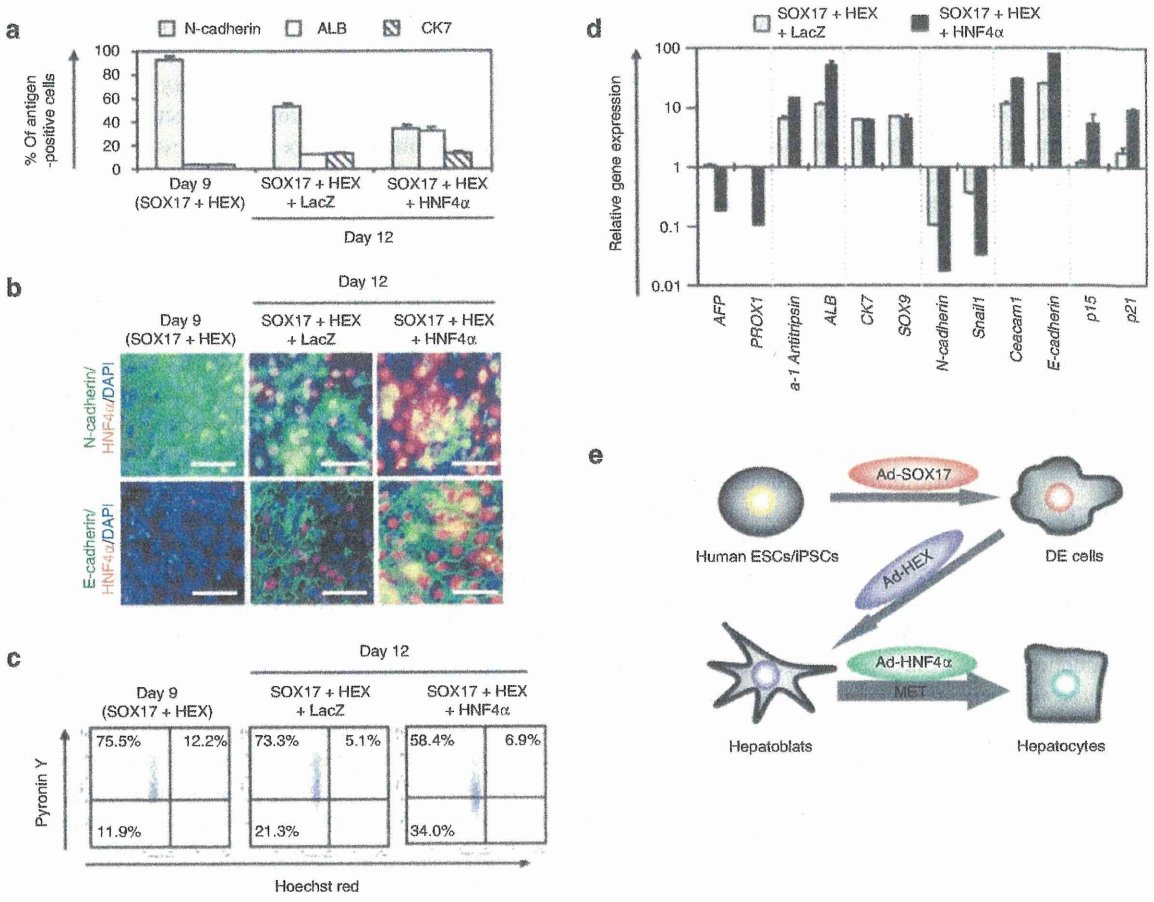

Figure 5 HNF4α promotes hepatic differentiation by activating MET. Human ESCs were differentiated into hepatoblasts according to the protocol described in **Figure 2a**, and then transduced with 3,000 VP/cell of Ad-LacZ or Ad-HNF4α for 1.5 hours, and finally cultured until day 12 of differentiation. (**a**) The hepatoblasts, two factors plus Ad-LacZ-transduced cells (SOX17+HEX+LacZ) (day 12), and the three factors-transduced cells (SOX17+HEX+HNF4α) (day 12) were subjected to immunostaining with anti-N-cadherin, ALB, or CK7 antibodies. The percentage of antigen-positive cells was measured by flow cytometry. (**b**) The cells were subjected to immunostaining with anti-N-cadherin (green), E-cadherin (green), or HNF4α (red) antibodies on day 9 or day 12 of differentiation. Nuclei were counterstained with DAPI (blue). The bar represents 50 μm. Similar results were obtained in two independent experiments. (**c**) The cell cycle was examined on day 9 or day 12 of differentiation. The cells were stained with Pyronin Y (y-axis) and Hoechst 33342 (x-axis) and then analyzed by flow cytometry. The growth fraction of cells is the population of actively dividing cells (G1/S/G2/M). (**d**) The expression levels of *AFP*, *PROX1*, *α-1-antitrypsin*, *ALB*, *CK7*, *SOX9*, *N-cadherin*, *Snail1*, *Ceacam1*, *E-cadherin*, *p15*, and *p21* were examined by real-time RT-PCR on day 9 or day 12 of differentiation. The expression level of hepatoblasts (day 9) was taken as 1.0. All data are represented as means ± SD ($n = 3$). (**e**) The model of efficient hepatic differentiation from human ESCs and iPSCs in this study is summarized. The human ESCs and iPSCs differentiate into hepatocytes via definitive endoderm and hepatoblasts. At each stage, the differentiation is promoted by stage-specific transduction of appropriate functional genes. In the last stage of hepatic differentiation, HNF4α transduction provokes hepatic maturation by activating MET. ESC, embryonic stem cell; HNF4α, hepatocyte nuclear factor 4α; iPSC, induced pluripotent stem cell; MET, mesenchymal-to-epithelial transition; RT-PCR, reverse transcription-PCR; VP, vector particle.

The gene expression levels of hepatocyte markers (*α-1-antitrypsin* and *ALB*)[20] and epithelial markers (*Ceacam1* and *E-cadherin*) were upregulated by HNF4α transduction. On the other hand, the gene expression levels of hepatoblast markers (*AFP* and *PROX1*)[31], mesenchymal markers (*N-cadherin* and *Snail*)[32], and cyclin dependent kinase inhibitor (*p15* and *p21*)[33] were downregulated by HNF4α transduction. HNF4α transduction did not change the expression levels of cholangiocyte markers (*CK7* and *SOX9*). We conclude that HNF4α promotes hepatic maturation by activating MET.

DISCUSSION

This study has two main purposes: the generation of functional hepatocytes from human ESCs and iPSCs for application to drug toxicity screening in the early phase of pharmaceutical development and; elucidation of the HNF4α function in hepatic maturation from human ESCs. We initially confirmed the importance of transcription factor HNF4α in hepatic differentiation from human ESCs by using a published data set of gene array analysis (**Supplementary Figure S1**).[34] We speculated that HNF4α transduction could enhance hepatic differentiation from human ESCs and iPSCs.

To generate functional hepatocytes from human ESCs and iPSCs and to elucidate the function of HNF4α in hepatic differentiation from human ESCs, we examined the stage-specific roles of HNF4α. We found that hepatoblast (day 9) stage-specific HNF4α transduction promoted hepatic differentiation (**Figure 1**). Because endogenous HNF4α is initially expressed in the hepatoblast,[9,10] our system might adequately reflect early embryogenesis. However, HNF4α transduction at an inappropriate stage (day 6 or day 12) promoted

bidirectional differentiation; heterogeneous populations, which contain the hepatocytes and pancreas cells or hepatocytes and cholangiocytes, were obtained, respectively (Figure 1), consistent with a previous report that HNF4α plays an important role not only in the liver but also in the pancreas.[12] Therefore, we concluded that HNF4α plays a significant stage-specific role in the differentiation of human ESC- and iPSC-derived hepatoblasts to hepatocytes (Figure 5e).

We found that the expression levels of the hepatic functional genes were upregulated by HNF4α transduction (Figure 3a,b, and **Supplementary Figures S7** and **S8**). Although the c/EBPα and GATA4 expression levels of the three factors-transduced cells were higher than those of primary human hepatocytes, the FOXA1, FOXA2, FOXA3, and HNF1α, which are known to be important for hepatic direct reprogramming and hepatic differentiation,[35,36] expression levels of three factors-transduced cells were slightly lower than those of primary human hepatocytes (**Supplementary Figure S8**). Therefore, additional transduction of FOXA1, FOXA2, FOXA3, and HNF1α might promote further hepatic maturation. Some previous hepatic differentiation protocols that utilized growth factors without gene transfer led to the appearance only of heterogeneous hepatocyte populations.[4–6] The HNF4α transduction led not only to the upregulation of expression levels of several hepatic markers but also to an almost homogeneous hepatocyte population; the differentiation efficacy based on CYPs, ASGR1, or ALB expression was ~80% (Figure 3c–e). The efficient hepatic maturation in this study might be attributable to the activation of many hepatocyte-associated genes by the transduction of HNF4α, which binds to the promoters of nearly half of the genes expressed in the liver.[12] In the later stage of hepatic maturation, hepatocyte-associated genes would be strongly upregulated by endogenous transcription factors but not exogenous HNF4α because transgene expression by Ad vectors was almost disappeared on day 18 (**Supplementary Figure S5**). Another reason for the efficient hepatic maturation would be that sequential transduction of SOX17, HEX, and HNF4α could mimic hepatic differentiation in early embryogenesis.

Next, we examined whether or not the hepatocyte-like cells had hepatic functions. The activity of many kinds of CYPs was upregulated by HNF4α transduction (Figure 4b). Ad-HNF4α-transduced cells exhibit many characteristics of hepatocytes: uptake of LDL, uptake and excretion of ICG, and storage of glycogen (Figure 4a,c,d). Many conventional tests of hepatic characteristics have shown that the hepatocyte-like cells have mature hepatocyte functions. Furthermore, the hepatocyte-like cells can catalyze the toxication of several compounds (Figure 4e). Although the activities to catalyze the toxication of test compounds in primary human hepatocytes are slightly higher than those in the hepatocyte-like cells, the handling of primary human hepatocytes is difficult for a number of reasons: since their source is limited, large-scale primary human hepatocytes are difficult to prepare as a homogeneous population. Therefore, the hepatocyte-like cells derived from human ESCs and iPSCs would be a valuable tool for predicting drug toxicity. To utilize the hepatocyte-like cells in a drug toxicity study, further investigation of the drug metabolism capacity and CYP induction potency will be needed.

We also investigated the mechanisms underlying efficient hepatic maturation by HNF4α transduction. Although the number of cholangiocyte populations did not change by HNF4α transduction, we found that the number of hepatoblast populations decreased and that of hepatocyte populations increased, indicating that HNF4α promotes selective hepatic differentiation from hepatoblasts (Figure 5a). As previously reported, HNF4α regulates the expression of a broad range of genes that code for cell adhesion molecules,[13] extracellular matrix components, and cytoskeletal proteins, which determine the main morphological characteristics of epithelial cells.[14,35,37] In this study, we elucidated that MET was promoted by HNF4α transduction (Figure 5b,d). Thus, we conclude that HNF4α overexpression in hepatoblasts promotes hepatic differentiation by activating MET (Figure 5e).

Using human iPSCs as well as human ESCs, we confirmed that the stage-specific overexpression of HNF4α could promote hepatic maturation (**Supplementary Figure S9**). Interestingly, the differentiation efficacies differed among human iPS cell lines: two of the human iPS cell lines (Dotcom and Tic) were more committed to the hepatic lineage than another human iPS cell line (201B7) (**Supplementary Figure S7**). Therefore, it would be necessary to select a human iPS cell line that is suitable for hepatic maturation in the case of medical applications, such as drug screening and liver transplantation. The difference of hepatic differentiation efficacy among the three iPSC lines might be due to the difference of epigenetic memory of original cells or the difference of the inserted position of the foreign genes for the reprogramming.

To control hepatic differentiation mimicking embryogenesis, we employed Ad vectors, which are one of the most efficient transient gene delivery vehicles and have been widely used in both experimental studies and clinical trials.[38] We used a fiber-modified Ad vector containing the EF-1α promoter and a stretch of lysine residue (KKKKKKK, K7) peptides in the C-terminal region of the fiber knob.[19] The K7 peptide targets heparan sulfates on the cellular surface, and the fiber-modified Ad vector containing the K7 peptides was shown to be efficient for transduction into many kinds of cells including human ESCs and human ESC-derived cells.[7–8,19] Thus, Ad vector-mediated transient gene transfer should be a powerful tool for regulating cellular differentiation.

In summary, the findings described here demonstrate that transcription factor HNF4α plays a crucial role in the hepatic differentiation from human ESC-derived hepatoblasts by activating MET (Figure 5e). In the present study, both human ESCs and iPSCs (three lines) were used and all cell lines showed efficient hepatic maturation, indicating that our protocol would be a universal tool for cell line-independent differentiation into functional hepatocytes. Moreover, the hepatocyte-like cells can catalyze the toxication of several compounds as primary human hepatocytes. Therefore, our technology, by sequential transduction of SOX17, HEX, and HNF4α, would be a valuable tool for the efficient generation of functional hepatocytes derived from human ESCs and iPSCs, and the hepatocyte-like cells could be used for the prediction of drug toxicity.

MATERIALS AND METHODS

Human ESC and iPSC culture. A human ES cell line, H9 (WiCell Research Institute, Madison, HI), was maintained on a feeder layer of mitomycin C-treated mouse embryonic fibroblasts (Millipore, Billerica, MA) with Repro Stem (Repro CELL, Tokyo, Japan) supplemented with 5ng/ml fibroblast

growth factor 2 (FGF2) (Sigma, St Louis, MO). Human ESCs were dissociated with 0.1 mg/ml dispase (Roche Diagnostics, Indianapolis, IN) into small clumps and then were subcultured every 4 or 5 days. H9 was used following the Guidelines for Derivation and Utilization of Human Embryonic Stem Cells of the Ministry of Education, Culture, Sports, Science and Technology of Japan. Two human iPS cell lines generated from the human embryonic lung fibroblast cell line MCR5 were provided from the JCRB Cell Bank (Tic, JCRB Number: JCRB1331; and Dotcom, JCRB Number: JCRB1327).[39,40] These human iPS cell lines were maintained on a feeder layer of mitomycin C-treated mouse embryonic fibroblasts with iPSellon (Cardio, Kobe, Japan) supplemented with 10 ng/ml FGF2. Another human iPS cell line, 201B7, generated from human dermal fibroblasts was kindly provided by Dr S. Yamanaka (Kyoto University).[2] The human iPS cell line 201B7 was maintained on a feeder layer of mitomycin C-treated mouse embryonic fibroblasts with Repro Stem (Repro CELL) supplemented with 5 ng/ml FGF2 (Sigma). Human iPSCs were dissociated with 0.1 mg/ml dispase (Roche Diagnostics) into small clumps and were then subcultured every 5 or 6 days.

In vitro *differentiation*. Before the initiation of cellular differentiation, the medium of human ESCs and iPSCs was exchanged for a defined serum-free medium, hESF9, and cultured as we previously reported.[41] hESF9 consists of hESF-GRO medium (Cell Science & Technology Institute, Sendai, Japan) supplemented with 10 μg/ml human recombinant insulin, 5 μg/ml human apotransferrin, 10 μmol/l 2-mercaptoethanol, 10 μmol/l ethanolamine, 10 μmol/l sodium selenite, oleic acid conjugated with fatty-acid-free bovine albumin (BSA), 10 ng/ml FGF2, and 100 ng/ml heparin (all from Sigma).

The differentiation protocol for the induction of DE cells, hepatoblasts, and hepatocytes was based on our previous report with some modifications.[7] Briefly, in mesendoderm differentiation, human ESCs and iPSCs were dissociated into single cells and cultured for 3 days on Matrigel (Becton, Dickinson and Company, Tokyo, Japan) in hESF-DIF medium (Cell Science & Technology Institute) supplemented with 10 μg/ml human recombinant insulin, 5 μg/ml human apotransferrin, 10 μmol/l 2-mercaptoethanol, 10 μmol/l ethanolamine, 10 μmol/l sodium selenite, 0.5 mg/ml BSA, and 100 ng/ml Activin A (R&D Systems, Minneapolis, MN). To generate mesendoderm cells and DE cells, human ESC-derived cells were transduced with 3,000 vector particles (VP)/cell of Ad-SOX17 for 1.5 hours on day 3 and cultured until day 6 on Matrigel (BD) in hESF-DIF medium (Cell Science & Technology Institute) supplemented with 10 μg/ml human recombinant insulin, 5 μg/ml human apotransferrin, 10 μmol/l 2-mercaptoethanol, 10 μmol/l ethanolamine, 10 μmol/l sodium selenite, 0.5 mg/ml BSA, and 100 ng/ml Activin A (R&D Systems). For induction of hepatoblasts, the DE cells were transduced with 3,000 VP/cell of Ad-HEX for 1.5 hours on day 6 and cultured for 3 days on a Matrigel (BD) in hESF-DIF (Cell Science & Technology Institute) medium supplemented with the 10 μg/ml human recombinant insulin, 5 μg/ml human apotransferrin, 10 μmol/l 2-mercaptoethanol, 10 μmol/l ethanolamine, 10 μmol/l sodium selenite, 0.5 mg/ml BSA, 20 ng/ml bone morphogenetic protein 4 (R&D Systems), and 20 ng/ml FGF4 (R&D Systems). In hepatic differentiation, hepatoblasts were transduced with 3,000 VP/cell of Ad-LacZ or Ad-HNF4α for 1.5 hr on day 9 and were cultured for 11 days on Matrigel (BD) in L15 medium (Invitrogen, Carlsbad, CA) supplemented with 8.3% tryptose phosphate broth (BD), 8.3% fetal bovine serum (Vita, Chiba, Japan), 10 μmol/l hydrocortisone 21-hemisuccinate (Sigma), 1 μmol/l insulin, 25 mmol/l $NaHCO_3$ (Wako, Osaka, Japan), 20 ng/ml hepatocyte growth factor (R&D Systems), 20 ng/ml Oncostatin M (R&D Systems), and 10^{-6} mol/l Dexamethasone (Sigma).

Ad vectors. Ad vectors were constructed by an improved *in vitro* ligation method.[42,43] The human HNF4α gene (accession number NM_000457) was amplified by PCR using primers designed to incorporate the 5′ Not I and 3′ Xba I restriction enzyme sites: Fwd 5′-ggcctctagatggaggcagggagaatg-3′ and Rev 5′-ccccgcggccgcagcggcttgctagataac-3′. The human HNF4α gene was inserted into pBSKII (Invitrogen), resulting in pBSKII-HNF4α, and then the human HNF4α gene was inserted into pHMEF5,[44] which contains the human elongation factor-1α (EF-1α) promoter, resulting in pHMEF-HNF4α. The pHMEF-HNF4α was digested with I-CeuI/PI-SceI and ligated into I-CeuI/PI-SceI-digested pAdHM41-K7,[19] resulting in pAd-HNF4α. The human EF-1α promoter-driven LacZ-, SOX17-, or HEX-expressing Ad vectors, Ad-LacZ, Ad-SOX17, or Ad-HEX, were constructed previously.[7,8,45] Ad-LacZ, Ad-SOX17, Ad-HEX, and Ad-HNF4α, each of which contains a stretch of lysine residue (K7) peptides in the C-terminal region of the fiber knob for more efficient transduction of human ESCs, iPSCs, and DE cells, were generated and purified as described previously.[7] The VP titer was determined by using a spectrophotometric method.[46]

LacZ assay. Human ESC- and iPSC-derived cells were transduced with Ad-LacZ at 3,000 VP/cell for 1.5 hours. After culturing for the indicated number of days, 5-bromo-4-chloro-3-indolyl β-D-galactopyranoside (X-Gal) staining was performed as described previously.[44]

Flow cytometry. Single-cell suspensions of human ESCs, iPSCs, and their derivatives were fixed with methanol at 4 °C for 20 minutes and then incubated with the primary antibody, followed by the secondary antibody. Flow cytometry analysis was performed using a FACS LSR Fortessa flow cytometer (BD).

RNA isolation and reverse transcription-PCR. Total RNA was isolated from human ESCs, iPSCs, and their derivatives using ISOGENE (Nippon Gene) according to the manufacturer's instructions. Primary human hepatocytes were purchased from CellzDirect, Durham, NC. complementary DNA was synthesized using 500 ng of total RNA with a Superscript VILO cDNA synthesis kit (Invitrogen). Real-time reverse transcription-PCR was performed with Taqman gene expression assays (Applied Biosystems, Foster City, CA) or SYBR Premix Ex Taq (TaKaRa) using an ABI PRISM 7000 Sequence Detector (Applied Biosystems). Relative quantification was performed against a standard curve and the values were normalized against the input determined for the housekeeping gene, glyceraldehyde 3-phosphate dehydrogenase. The primer sequences used in this study are described in **Supplementary Table S1.**

Immunohistochemistry. The cells were fixed with methanol or 4% paraformaldehyde (Wako). After blocking with phosphate-buffered saline containing 2% BSA (Sigma) and 0.2% Triton X-100 (Sigma), the cells were incubated with primary antibody at 4 °C for 16 hours, followed by incubation with a secondary antibody that was labeled with Alexa Fluor 488 (Invitrogen) or Alexa Fluor 594 (Invitrogen) at room temperature for 1 hour. All the antibodies are listed in **Supplementary Table S2.**

Assay for CYP activity. To measure cytochrome P450 3A4, 2C9, and 1A2 activity, we performed Lytic assays by using a P450-GloTM CYP3A4 Assay Kit (Promega, Madison, WI). For the CYP3A4 and 2C9 activity assay, undifferentiated human ESCs, the hepatocyte-like cells, and primary human hepatocytes were treated with rifampicin (Sigma), which is the substrate for CYP3A4 and CYP2C9, at a final concentration of 25 μmol/l or DMSO (0.1%) for 48 hours. For the CYP1A2 activity assay, undifferentiated human ESCs, the hepatocyte-like cells, and primary human hepatocytes were treated with omeprazole (Sigma), which is the substrate for CYP1A2, at a final concentration of 10 μM or DMSO (0.1%) for 48 hours. We measured the fluorescence activity with a luminometer (Lumat LB 9507; Berthold, Oak Ridge, TN) according to the manufacturer's instructions.

Pyronin Y/Hoechst Staining. Human ESC-derived cells were stained with Hoechst33342 (Sigma) and Pyronin Y (PY) (Sigma) in Dulbecco's modified Eagle medium (Wako) supplemented with 0.2 mmol/l HEPES and 5% FCS (Invitrogen). Samples were then placed on ice for 15 minutes, and 7-AAD was added to a final concentration of 0.5 mg/ml for exclusion of dead cells. Fluorescence-activated cell-sorting analysis of these cells was

performed on a FACS LSR Fortessa flow cytometer (Becton Dickinson) equipped with a UV-laser.

Cellular uptake and excretion of ICG. ICG (Sigma) was dissolved in DMSO at 100 mg/ml, then added to a culture medium of the hepatocyte-like cells to a final concentration of 1 mg/ml on day 20 of differentiation. After incubation at 37°C for 60 minutes, the medium with ICG was discarded and the cells were washed with phosphate-buffered saline. The cellular uptake of ICG was then examined by microscopy. Phosphate-buffered saline was then replaced by the culture medium and the cells were incubated at 37°C for 6 hours. The excretion of ICG was examined by microscopy.

Periodic Acid-Schiff assay for glycogen. The hepatocyte-like cells were fixed with 4% paraformaldehyde and stained using a Periodic Acid-Schiff staining system (Sigma) on day 20 of differentiation according to the manufacturer's instructions.

Cell viability tests. Cell viability was assessed by Alamar Blue assay kit (Invitrogen). After treatment with test compounds[47–50] (troglitazone, acetaminophen, cyclophosphamide, and carbamazepine) (all from Wako) for 2 days, the culture medium was replaced with 0.5 mg/ml solution of Alamar Blue in culturing medium and cells were incubated for 3 hours at 37°C. The supernatants of the cells were measured at a wavelength of 570 nm with background subtraction at 600 nm in a plate reader. Control refers to incubations in the absence of test compounds and was considered as 100% viability value.

Uptake of LDL. The hepatocyte-like cells were cultured with medium containing Alexa-488-labeled LDL (Invitrogen) for 1 hour, and then the cells that could uptake LDL were assessed by immunohistochemistry and flow cytometry.

Primary human hepatocytes. Cryopreserved human hepatocytes were purchased from CellzDirect (lot Hu8072). The vials of hepatocytes were rapidly thawed in a shaking water bath at 37°C; the contents of the vial were emptied into prewarmed Cryopreserved Hepatocyte Recovery Medium (CellzDirect) and the suspension was centrifuged at 100*g* for 10 minutes at room temperature. The hepatocytes were seeded at 1.25×10^5 cells/cm^2 in hepatocyte culture medium (Lonza, Walkersville, MD) containing 10% FCS (GIBCO-BRL) onto type I collagen-coated 12-well plates. The medium was replaced with hepatocyte culture medium containing 10% FCS (GIBCO-BRL) 6 hours after seeding. The hepatocytes, which were cultured 48 hours after plating the cells, were used in the experiments.

SUPPLEMENTARY MATERIAL

Figure S1. Genome-wide screening of transcription factors involved in hepatic differentiation emphasizes the importance of the transcription factor HNF4α.
Figure S2. Summary of specific markers for DE cells, hepatoblasts, hepatocytes, cholangiocytes, and pancreas cells.
Figure S3. The formation of DE cells, hepatoblasts, hepatocytes, and cholangiocytes from human ESCs.
Figure S4. Overexpression of HNF4α mRNA in hepatoblasts by Ad-HNF4α transduction.
Figure S5. Time course of LacZ expression in hepatoblasts transduced with Ad-LacZ.
Figure S6. The morphology of the hepatocyte-like cells.
Figure S7. Upregulation of the expression levels of conjugating enzymes and hepatic transporters by HNF4α transduction.
Figure S8. Upregulation of the expression levels of hepatic transcription factors by HNF4α transduction.
Figure S9. Generation of hepatocytes from various human ES or iPS cell lines.
Figure S10. Promotion of MET by HNF4α transduction.
Figure S11. Arrest of cell growth by HNF4α transduction.
Table S1. List of Taqman probes and primers used in this study.
Table S2. List of antibodies used in this study.

ACKNOWLEDGMENTS

We thank Hiroko Matsumura and Misae Nishijima for their excellent technical support. H.M., M.K.F., and T.H. were supported by grants from the Ministry of Health, Labor, and Welfare of Japan. H.M. was also supported by Japan Research foundation For Clinical Phamacology, The Nakatomi Foundation, and The Uehara Memorial Foundation. K.K. (K. Kawabata) was supported by grants from the Ministry of Education, Sports, Science and Technology of Japan (20200076) and the Ministry of Health, Labor, and Welfare of Japan. K.K. (K. Katayama) and F.S. was supported by Program for Promotion of Fundamental Studies in Health Sciences of the National Institute of Biomedical Innovation (NIBIO).

REFERENCES

1. Thomson, JA, Itskovitz-Eldor, J, Shapiro, SS, Waknitz, MA, Swiergiel, JJ, Marshall, VS *et al.* (1998). Embryonic stem cell lines derived from human blastocysts. *Science* **282**: 1145–1147.
2. Takahashi, K, Tanabe, K, Ohnuki, M, Narita, M, Ichisaka, T, Tomoda, K *et al.* (2007). Induction of pluripotent stem cells from adult human fibroblasts by defined factors. *Cell* **131**: 861–872.
3. Murry, CE and Keller, G (2008). Differentiation of embryonic stem cells to clinically relevant populations: lessons from embryonic development. *Cell* **132**: 661–680.
4. Basma, H, Soto-Gutiérrez, A, Yannam, GR, Liu, L, Ito, R, Yamamoto, T *et al.* (2009). Differentiation and transplantation of human embryonic stem cell-derived hepatocytes. *Gastroenterology* **136**: 990–999.
5. Touboul, T, Hannan, NR, Corbineau, S, Martinez, A, Martinet, C, Branchereau, S *et al.* (2010). Generation of functional hepatocytes from human embryonic stem cells under chemically defined conditions that recapitulate liver development. *Hepatology* **51**: 1754–1765.
6. Duan, Y, Ma, X, Ma, X, Zou, W, Wang, C, Bahbahan, IS *et al.* (2010). Differentiation and characterization of metabolically functioning hepatocytes from human embryonic stem cells. *Stem Cells* **28**: 674–686.
7. Inamura, M, Kawabata, K, Takayama, K, Tashiro, K, Sakurai, F, Katayama, K *et al.* (2011). Efficient generation of hepatoblasts from human ES cells and iPS cells by transient overexpression of homeobox gene HEX. *Mol Ther* **19**: 400–407.
8. Takayama, K, Inamura, M, Kawabata, K, Tashiro, K, Katayama, K, Sakurai, F *et al.* (2011). Efficient and directive generation of two distinct endoderm lineages from human ESCs and iPSCs by differentiation stage-specific SOX17 transduction. *PLoS ONE* **6**: e21780.
9. Duncan, SA, Manova, K, Chen, WS, Hoodless, P, Weinstein, DC, Bachvarova, RF *et al.* (1994). Expression of transcription factor HNF-4 in the extraembryonic endoderm, gut, and nephrogenic tissue of the developing mouse embryo: HNF-4 is a marker for primary endoderm in the implanting blastocyst. *Proc Natl Acad Sci USA* **91**: 7598–7602.
10. Taraviras, S, Monaghan, AP, Schütz, G and Kelsey, G (1994). Characterization of the mouse HNF-4 gene and its expression during mouse embryogenesis. *Mech Dev* **48**: 67–79.
11. Parviz, F, Matullo, C, Garrison, WD, Savatski, L, Adamson, JW, Ning, G *et al.* (2003). Hepatocyte nuclear factor 4alpha controls the development of a hepatic epithelium and liver morphogenesis. *Nat Genet* **34**: 292–296.
12. Odom, DT, Zizlsperger, N, Gordon, DB, Bell, GW, Rinaldi, NJ, Murray, HL *et al.* (2004). Control of pancreas and liver gene expression by HNF transcription factors. *Science* **303**: 1378–1381.
13. Battle, MA, Konopka, G, Parviz, F, Gaggl, AL, Yang, C, Sladek, FM *et al.* (2006). Hepatocyte nuclear factor 4alpha orchestrates expression of cell adhesion proteins during the epithelial transformation of the developing liver. *Proc Natl Acad Sci USA* **103**: 8419–8424.
14. Konopka, G, Tekiela, J, Iverson, M, Wells, C and Duncan, SA (2007). Junctional adhesion molecule-A is critical for the formation of pseudocanaliculi and modulates E-cadherin expression in hepatic cells. *J Biol Chem* **282**: 28137–28148.
15. Li, J, Ning, G and Duncan, SA (2000). Mammalian hepatocyte differentiation requires the transcription factor HNF-4alpha. *Genes Dev* **14**: 464–474.
16. Hayhurst, GP, Lee, YH, Lambert, G, Ward, JM and Gonzalez, FJ (2001). Hepatocyte nuclear factor 4alpha (nuclear receptor 2A1) is essential for maintenance of hepatic gene expression and lipid homeostasis. *Mol Cell Biol* **21**: 1393–1403.
17. Khurana, S, Jaiswal, AK and Mukhopadhyay, A (2010). Hepatocyte nuclear factor-4alpha induces transdifferentiation of hematopoietic cells into hepatocytes. *J Biol Chem* **285**: 4725–4731.
18. Suetsugu, A, Nagaki, M, Aoki, H, Motohashi, T, Kunisada, T and Moriwaki, H (2008). Differentiation of mouse hepatic progenitor cells induced by hepatocyte nuclear factor-4 and cell transplantation in mice with liver fibrosis. *Transplantation* **86**: 1178–1186.
19. Koizumi, N, Mizuguchi, H, Utoguchi, N, Watanabe, Y and Hayakawa, T (2003). Generation of fiber-modified adenovirus vectors containing heterologous peptides in both the HI loop and C terminus of the fiber knob. *J Gene Med* **5**: 267–276.
20. Shiojiri, N (1984). The origin of intrahepatic bile duct cells in the mouse. *J Embryol Exp Morphol* **79**: 25–39.
21. Moll, R, Franke, WW, Schiller, DL, Geiger, B and Krepler, R (1982). The catalog of human cytokeratins: patterns of expression in normal epithelia, tumors and cultured cells. *Cell* **31**: 11–24.

22. Antoniou, A, Raynaud, P, Cordi, S, Zong, Y, Tronche, F, Stanger, BZ *et al.* (2009). Intrahepatic bile ducts develop according to a new mode of tubulogenesis regulated by the transcription factor SOX9. *Gastroenterology* **136**: 2325–2333.
23. Offield, MF, Jetton, TL, Labosky, PA, Ray, M, Stein, RW, Magnuson, MA *et al.* (1996). PDX-1 is required for pancreatic outgrowth and differentiation of the rostral duodenum. *Development* **122**: 983–995.
24. Sussel, L, Kalamaras, J, Hartigan-O'Connor, DJ, Meneses, JJ, Pedersen, RA, Rubenstein, JL *et al.* (1998). Mice lacking the homeodomain transcription factor Nkx2.2 have diabetes due to arrested differentiation of pancreatic beta cells. *Development* **125**: 2213–2221.
25. Ingelman-Sundberg, M, Oscarson, M and McLellan, RA (1999). Polymorphic human cytochrome P450 enzymes: an opportunity for individualized drug treatment. *Trends Pharmacol Sci* **20**: 342–349.
26. Henderson, CJ, Otto, DM, Carrie, D, Magnuson, MA, McLaren, AW, Rosewell, I *et al.* (2003). Inactivation of the hepatic cytochrome P450 system by conditional deletion of hepatic cytochrome P450 reductase. *J Biol Chem* **278**: 13480–13486.
27. Yamada, T, Yoshikawa, M, Kanda, S, Kato, Y, Nakajima, Y, Ishizaka, S *et al.* (2002). *In vitro* differentiation of embryonic stem cells into hepatocyte-like cells identified by cellular uptake of indocyanine green. *Stem Cells* **20**: 146–154.
28. Anzenbacher, P and Anzenbacherová, E (2001). Cytochromes P450 and metabolism of xenobiotics. *Cell Mol Life Sci* **58**: 737–747.
29. Zhao, D, Chen, S, Cai, J, Guo, Y, Song, Z, Che, J *et al.* (2009). Derivation and characterization of hepatic progenitor cells from human embryonic stem cells. *PLoS ONE* **4**: e6468.
30. Hatta, K, Takagi, S, Fujisawa, H and Takeichi, M (1987). Spatial and temporal expression pattern of N-cadherin cell adhesion molecules correlated with morphogenetic processes of chicken embryos. *Dev Biol* **120**: 215–227.
31. Shiojiri, N (1981). Enzymo- and immunocytochemical analyses of the differentiation of liver cells in the prenatal mouse. *J Embryol Exp Morphol* **62**: 139–152.
32. Lee, JM, Dedhar, S, Kalluri, R and Thompson, EW (2006). The epithelial-mesenchymal transition: new insights in signaling, development, and disease. *J Cell Biol* **172**: 973–981.
33. Macleod, KF, Sherry, N, Hannon, G, Beach, D, Tokino, T, Kinzler, K *et al.* (1995). p53-dependent and independent expression of p21 during cell growth, differentiation, and DNA damage. *Genes Dev* **9**: 935–944.
34. Si-Tayeb, K, Noto, FK, Nagaoka, M, Li, J, Battle, MA, Duris, C *et al.* (2010). Highly efficient generation of human hepatocyte-like cells from induced pluripotent stem cells. *Hepatology* **51**: 297–305.
35. Sekiya, S and Suzuki, A (2011). Direct conversion of mouse fibroblasts to hepatocyte-like cells by defined factors. *Nature* **475**: 390–393.
36. Huang, P, He, Z, Ji, S, Sun, H, Xiang, D, Liu, C *et al.* (2011). Induction of functional hepatocyte-like cells from mouse fibroblasts by defined factors. *Nature* **475**: 386–389.
37. Satohisa, S, Chiba, H, Osanai, M, Ohno, S, Kojima, T, Saito, T *et al.* (2005). Behavior of tight-junction, adherens-junction and cell polarity proteins during HNF-4alpha-induced epithelial polarization. *Exp Cell Res* **310**: 66–78.
38. Xu, ZL, Mizuguchi, H, Sakurai, F, Koizumi, N, Hosono, T, Kawabata, K *et al.* (2005). Approaches to improving the kinetics of adenovirus-delivered genes and gene products. *Adv Drug Deliv Rev* **57**: 781–802.
39. Nagata, S, Toyoda, M, Yamaguchi, S, Hirano, K, Makino, H, Nishino, K *et al.* (2009). Efficient reprogramming of human and mouse primary extra-embryonic cells to pluripotent stem cells. *Genes Cells* **14**: 1395–1404.
40. Makino, H, Toyoda, M, Matsumoto, K, Saito, H, Nishino, K, Fukawatase, Y *et al.* (2009). Mesenchymal to embryonic incomplete transition of human cells by chimeric OCT4/3 (POU5F1) with physiological co-activator EWS. *Exp Cell Res* **315**: 2727–2740.
41. Furue, MK, Na, J, Jackson, JP, Okamoto, T, Jones, M, Baker, D *et al.* (2008). Heparin promotes the growth of human embryonic stem cells in a defined serum-free medium. *Proc Natl Acad Sci USA* **105**: 13409–13414.
42. Mizuguchi, H and Kay, MA (1998). Efficient construction of a recombinant adenovirus vector by an improved *in vitro* ligation method. *Hum Gene Ther* **9**: 2577–2583.
43. Mizuguchi, H and Kay, MA (1999). A simple method for constructing E1- and E1/E4-deleted recombinant adenoviral vectors. *Hum Gene Ther* **10**: 2013–2017.
44. Kawabata, K, Sakurai, F, Yamaguchi, T, Hayakawa, T and Mizuguchi, H (2005). Efficient gene transfer into mouse embryonic stem cells with adenovirus vectors. *Mol Ther* **12**: 547–554.
45. Tashiro, K, Kawabata, K, Sakurai, H, Kurachi, S, Sakurai, F, Yamanishi, K *et al.* (2008). Efficient adenovirus vector-mediated PPAR gamma gene transfer into mouse embryoid bodies promotes adipocyte differentiation. *J Gene Med* **10**: 498–507.
46. Maizel, JV Jr, White, DO and Scharff, MD (1968). The polypeptides of adenovirus. I. Evidence for multiple protein components in the virion and a comparison of types 2, 7A, and 12. *Virology* **36**: 115–125.
47. Smith, MT (2003). Mechanisms of troglitazone hepatotoxicity. *Chem Res Toxicol* **16**: 679–687.
48. Dai, Y and Cederbaum, AI (1995). Cytotoxicity of acetaminophen in human cytochrome P4502E1-transfected HepG2 cells. *J Pharmacol Exp Ther* **273**: 1497–1505.
49. Chang, TK, Weber, GF, Crespi, CL and Waxman, DJ (1993). Differential activation of cyclophosphamide and ifosphamide by cytochromes P-450 2B and 3A in human liver microsomes. *Cancer Res* **53**: 5629–5637.
50. Miao, XS and Metcalfe, CD (2003). Determination of carbamazepine and its metabolites in aqueous samples using liquid chromatography-electrospray tandem mass spectrometry. *Anal Chem* **75**: 3731–3738.

Research Article

EASL EUROPEAN ASSOCIATION FOR THE STUDY OF THE LIVER | JOURNAL OF HEPATOLOGY

Generation of metabolically functioning hepatocytes from human pluripotent stem cells by FOXA2 and HNF1α transduction

Kazuo Takayama[1,2], Mitsuru Inamura[1,2], Kenji Kawabata[2,3], Michiko Sugawara[4], Kiyomi Kikuchi[4], Maiko Higuchi[2], Yasuhito Nagamoto[1,2], Hitoshi Watanabe[1,2], Katsuhisa Tashiro[2], Fuminori Sakurai[1], Takao Hayakawa[5,6], Miho Kusuda Furue[7,8], Hiroyuki Mizuguchi[1,2,9,*]

[1]*Laboratory of Biochemistry and Molecular Biology, Graduate School of Pharmaceutical Sciences, Osaka University, Osaka 565-0871, Japan;* [2]*Laboratory of Stem Cell Regulation, National Institute of Biomedical Innovation, Osaka 567-0085, Japan;* [3]*Laboratory of Biomedical Innovation, Graduate School of Pharmaceutical Sciences, Osaka University, Osaka 565-0871, Japan;* [4]*Tsukuba Laboratories, Eisai Co., Ltd., Ibaraki 300-2635, Japan;* [5]*Pharmaceutics and Medical Devices Agency, Tokyo 100-0013, Japan;* [6]*Pharmaceutical Research and Technology Institute, Kinki University, Osaka 577-8502, Japan;* [7]*Laboratory of Cell Cultures, Department of Disease Bioresources Research, National Institute of Biomedical Innovation, Osaka 567-0085, Japan;* [8]*Laboratory of Cell Processing, Institute for Frontier Medical Sciences, Kyoto University, Kyoto 606-8507, Japan;* [9]*The Center for Advanced Medical Engineering and Informatics, Osaka University, Osaka 565-0871, Japan*

Background & Aims: Hepatocyte-like cells differentiated from human embryonic stem cells (hESCs) and induced pluripotent stem cells (hiPSCs) can be utilized as a tool for screening for hepatotoxicity in the early phase of pharmaceutical development. We have recently reported that hepatic differentiation is promoted by sequential transduction of SOX17, HEX, and HNF4α into hESC- or hiPSC-derived cells, but further maturation of hepatocyte-like cells is required for widespread use of drug screening.
Methods: To screen for hepatic differentiation-promoting factors, we tested the seven candidate genes related to liver development.
Results: The combination of two transcription factors, FOXA2 and HNF1α, promoted efficient hepatic differentiation from hESCs and hiPSCs. The expression profile of hepatocyte-related genes (such as genes encoding cytochrome P450 enzymes, conjugating enzymes, hepatic transporters, and hepatic nuclear receptors) achieved with FOXA2 and HNF1α transduction was comparable to that obtained in primary human hepatocytes. The hepatocyte-like cells generated by FOXA2 and HNF1α transduction exerted various hepatocyte functions including albumin and urea secretion, and the uptake of indocyanine green and low density lipoprotein. Moreover, these cells had the capacity to metabolize all nine tested drugs and were successfully employed to evaluate drug-induced cytotoxicity.
Conclusions: Our method employing the transduction of FOXA2 and HNF1α represents a useful tool for the efficient generation of metabolically functional hepatocytes from hESCs and hiPSCs, and the screening of drug-induced cytotoxicity.

Keywords: FOXA2; HNF1α; Hepatocytes; Adenovirus; Drug screening; Drug metabolism; hESCs; hiPSCs.
Received 14 November 2011; received in revised form 31 March 2012; accepted 4 April 2012; available online 29 May 2012
* Corresponding author. Address: Laboratory of Biochemistry and Molecular Biology, Graduate School of Pharmaceutical Sciences, Osaka University, 1-6 Yamadaoka, Suita, Osaka 565-0871, Japan. Tel.: +81 6 6879 8185; fax: +81 6 6879 8186.
E-mail address: mizuguch@phs.osaka-u.ac.jp (H. Mizuguchi).

Introduction

Hepatocyte-like cells differentiated from human embryonic stem cells (hESCs) [1] or human induced pluripotent stem cells (hiPSCs) [2] have more advantages than primary human hepatocytes (PHs) for drug screening. While application of PHs in drug screening has been hindered by lack of cellular growth, loss of function, and de-differentiation *in vitro* [3], hESC- or hiPSC-derived hepatocyte-like cells (hESC-hepa or hiPSC-hepa, respectively) have potential to solve these problems.

Hepatic differentiation from hESCs and hiPSCs can be divided into four stages: definitive endoderm (DE) differentiation, hepatic commitment, hepatic expansion, and hepatic maturation. Various growth factors are required to mimic liver development [4] and to promote hepatic differentiation. Previously, we showed that transduction of transcription factors in addition to treatment with optimal growth factors was effective to enhance hepatic differentiation [5–7]. An almost homogeneous hepatocyte population was obtained by sequential transduction of SOX17, HEX, and HNF4α into hESC- or hiPSCs-derived cells [7]. However, further maturation of the hESC-hepa and hiPSC-hepa is required for widespread use of drug screening because the drug metabolism capacity of these cells was not sufficient.

In some previous reports, hESC-hepa and hiPSC-hepa have been characterized for their hepatocyte functions in numerous ways, including functional assessment such as glycogen storage and low density lipoprotein (LDL) uptake [7]. To make a more precise judgment as to whether hESC-hepa and hiPSC-hepa can be applied to drug screening, it is more important to assess cytochrome P450 (CYP) induction potency and drug metabolism capacity rather than general hepatocyte function. Although Duan *et al.* have examined the drug metabolism capacity of hESC-hepa, drug metabolites were measured at 24 or 48 h [8]. To precisely